Stanford Accelerated Intelligent Neuromodulation Therapy (SAINT) Induces Functional Connectivity Changes in Emotion Regulation Brain Areas for MDD Patients

Xiaoqian Xiao[1#], Brandon S. Bentzley[1#], Eleanor Cole, Claudia Tischler, Katy H. Stimpson, Dalton Duvio, James Bishop[2], Alan Schatzberg, Corey Keller, Keith Sudheimer*[1&], Nolan R. Williams*[1&]

[#]Co-first authors

*Corresponding Authors

[&]Co-Senior Authors

[1]Department of Psychiatry & Behavioral Sciences, Stanford University, Palo Alto, California, USA.

[2]Department of Radiology, Stanford University, Palo Alto, California, USA.

Corresponding Authors:
Nolan Williams, MD
Keith Sudheimer, PhD
401 Quarry Road
Room 2360
Palo Alto, CA 94304
(650) 498-9111
nolanw@stanford.edu

NRW and KDS have filed intellectual property on the methodology discussed in this manuscript.

Trial registration: ClinicalTrials.gov NCT03240692

Acknowledgements: The authors kindly thank the following for supporting this study: Charles R. Schwab, The Marshall and Dee Ann Payne Fund, the Lehman Family, Neuromodulation Research Fund, Still Charitable Fund, Avy L. and Robert L. Miller Foundation, Stanford Psychiatry Chairman's Small Grant, Stanford CNI Innovation Award, NIH T32 035165, NIH UL1 TR001085, Stanford Medical Scholars Research Scholarship, NARSAD Young Investigator Award, the Gordie Brookstone Fund, and the Stanford Department of Psychiatry & Behavioral Sciences.

Abbreviations: AI: anterior insula, BA: basolateral amygdala, CMA: centromedian amygdala, dACC: dorsal anterior cingulate cortex, DLPFC: dorsolateral prefrontal cortex, DMN: default mode network, exeS: executive striatum, fc: functional connectivity, HAMD: Hamilton Depression Rating Scale, Ins: insula, limS: limbic striatum, MADRS: Montgomery Asberg Depression Rating Scale, MDD: major depressive disorder, SA: superficial amygdala, sgACC: subgenual anterior cingulate cortex, SN: salience network, VLPFC: ventrolateral prefrontal cortex. Preceding r: right, preceding l: left.

Abstract

Background: Major depressive disorder (MDD) is prevalent and debilitating, and development of improved treatments is limited in part by insufficient understanding of the mechanism of disease remission. In turn, efforts to elucidate mechanisms have been challenging due to disease heterogeneity and limited effectiveness of treatments, which require weeks-to-months to induce remission. We recently developed a form of repetitive transcranial magnetic stimulation that induces remission in 90% of individuals with severe, treatment resistant MDD in 1-5 days (SAINT). This provides a new tool to begin exploring the network-level mechanisms of MDD remission.

Objective: Determine the functional connectivity (fc) changes that occur with SAINT in brain regions associated with emotion regulation.

Methods: Resting-state fMRI scans were performed just prior to (baseline), and following, open-label SAINT in 18 participants with severe, treatment-resistant MDD. Fc was determined between regions of interest (ROIs) defined a priori with well-described roles in emotion regulation.

Results: Following SAINT treatment fc was significantly decreased between the following ROI pairs: dorsolateral prefrontal cortex (DLPFC)-striatum, DLPFC-amygdala, default mode network (DMN)-subgenual cingulate cortex (sgACC), DMN-amygdala, DMN-striatum, amygdala-striatum, and between amygdala subregions. Greater clinical improvements were associated with larger decreases in fc between DLPFC-amygdala and DLPFC-insula. Greater clinical improvements were associated with smaller decreases in fc between sgACC-DMN. Significant increases and decreases in fc between insula-amygdala were observed depending on the subregions. Greater clinical improvements were associated with lower baseline fc between DMN-DLPFC, DMN-striatum, and DMN-ventrolateral prefrontal cortex.

Conclusion: SAINT-induced remission from depression is associated with fc changes that suggest improved regulation of emotion. Although preliminary, this leads us to hypothesize that interventions that augment top-down regulation of emotion may be effective depression treatments.

Introduction

Major depressive disorder (MDD) is the leading cause of disability worldwide (Friedrich, 2017; World Health Organization, 2017) and is increasingly common, with lifetime prevalence in the United States now more than 20% (Hasin et al., 2018). Combating this endemic disease will require improvements in prophylaxis and treatments; however, development of both is limited in part by insufficient understanding of the mechanism of disease remission.

Discovering the network-level mechanisms of remission has been particularly challenging due to MDD treatments requiring weeks-to-months to induce remission (Trivedi et al., 2006), limited effectiveness of available treatments (Heijnen et al., 2010; Rush et al., 2006), and potential disease heterogeneity (Dinga et al., 2018; Drysdale et al., 2017). We recently developed a form of repetitive transcranial magnetic stimulation (rTMS) that induces remission in 90% of individuals with severe, treatment-resistant MDD within 1-5 days (SAINT) (Cole et al., 2019; Williams et al., 2018). Given that the majority of patients' depressive symptoms remit rapidly, SAINT provides a new opportunity to begin investigating the network alterations underlying MDD remission.

Neuroimaging-based approaches that assess resting-state functional connectivity (fc) have demonstrated some success in investigating neurocircuit-level dysfunction of MDD. These approaches have been used to investigate neurophysiological subtypes of MDD (Dinga et al., 2018; Drysdale et al., 2017) and predict treatment efficacy of rTMS (Avissar et al., 2017; Baeken et al., 2014; Drysdale et al., 2017; Du et al., 2018; Fox et al., 2012a; Siddiqi et al., 2019; Weigand et al., 2018; Cash et al., 2019). Given the promise of this approach, we performed resting state fc analyses on participants before and after SAINT. For this initial investigation, we restricted our analysis to brain regions involved in emotion regulation.

Several lines of evidence suggest dysfunction of emotion regulation in MDD (Joormann and Vanderlind, 2014) with neural correlates observed with fMRI (Rive et al., 2013; Sheline et al., 2009). The neural basis of emotion regulation includes emotional reactivity: amygdala and striatum; explicit control of emotion – central executive network (CEN): dorsolateral prefrontal cortex (dlPFC), ventrolateral PFC (vlPFC); and implicit emotion regulation – default mode network (DMN), salience affective network (SN) and insula. For review, see Etkin et al. (2015). Specifically, dysfunction within the DMN, CEN, and SN has repeatedly been reported in individuals with MDD (Greicius et al., 2007; Hamilton et al., 2015; Liston et al., 2014; Sheline et al., 2010; Wise et al., 2017). Numerous fMRI studies have demonstrated that individuals with MDD have altered frontal connectivity with amygdala (Almeida et al., 2009; Beauregard et al., 2006; Erk et al., 2010; Greening et al., 2014; Stephanou et al., 2017) and striatum (Avissar et al., 2017; Furman et al., 2011; Pan et al., 2017; Redlich

et al., 2015); hyperconnectivity between DMN and amygdala (de Kwaasteniet et al., 2013; Li et al., 2015; Pannekoek et al., 2014; Peters et al., 2016); and alterations in insular connectivity with multiple nodes (Connolly et al., 2017; Kaiser et al., 2016; Peters et al., 2016).

Following the emotional dysregulation hypothesis of depression, stimulation of the CEN at the lDLPFC node via rTMS (De Raedt et al., 2010; Lantrip et al., 2017; Liston et al., 2014) and transcranial direct current stimulation (Wolkenstein and Plewnia, 2013) has been hypothesized to produce antidepressant effects via enhanced regulation of emotion. This is in line with Chen et al's seminal interleaved TMS/fMRI study demonstrating causal interactions between CEN and DMN, such that increased activity in CEN results in suppression of DMN (Chen et al., 2013), and this has led others to hypothesize that improved accuracy of targeting these networks might produce better treatment efficacy (Cash et al., 2019; Fischer et al., 2016; Fox et al., 2012b; Luber et al., 2017; Siddiqi et al., 2019; Weigand et al., 2018). However, if potentiation of CEN and consequent suppression of DMN accounts for the primary antidepressant mechanism of rTMS of the lDLPFC, then it remains unclear why clinical trials demonstrate that only a third or less of participants remit from their depressive episode with rTMS treatment (George et al., 2010; Levkovitz et al., 2015; O'Reardon et al., 2007). We hypothesized that individualized targeting and enhanced stimulation techniques could improve outcomes (Williams et al., 2018), and in our initial open-label trial of SAINT in patients with severe, treatment-resistant depression, we observed a strikingly high remission rate of 90% with a mean of 3 days of treatment to produce remision (Cole et al., 2019). Thus, fc changes that occur with SAINT may reflect generalized network-level changes associated with remission from depression. Herein, we report our first investigation of the resting-state fc changes that occur in brain regions associated with emotion regulation in participants with MDD undergoing open-label SAINT.

Materials and Methods

Participants

Detailed information regarding participants, the SAINT protocol, experimental design, and behavioral data analysis can be found in our previously published report (Cole et al., 2019). Briefly, 19 participants treated with SAINT had a diagnosis of treatment-resistant MDD [9 males, age 50.11±14.58 (mean±SD) range 20-78 years] and complete MRI scans both pre- and post-SAINT. Diagnosis of MDD was confirmed with the Mini International Neuropsychiatric Interview (MINI). Participants were required to have a Hamilton Depression Rating Scale 17-item (HDRS-17) score higher than 20 and not have responded to at least one antidepressant medication (minimum trial duration of six weeks) to be eligible for the study. Participants had no history of a psychotic disorder, substance use disorder, major systemic illness, current mania (assessed using the Young

Mania Rating Scale), lesional neurological disorder, or any contraindications to rTMS or MRI (such as implanted metal or history of seizures). All participants provided written informed consent, and the study was approved by the Stanford University Institutional Review Board and in accordance to the Declaration of Helsinki.

Stanford Accelerated Intelligent Neuromodulation Therapy (SAINT)

Participants received a five-day treatment course under the SAINT protocol. Stimulation location was chosen based on an algorithm that selected the area within the left dorsolateral prefrontal cortex (lDLPFC) with the most negative fc with sgACC. This is described in detail in our prior report (Cole et al., 2019). A Magventure Magpro X100 (MagVenture A/S, Denmark) system was used to deliver sessions of intermittent theta-burst stimulation (iTBS): 60 cycles of 10 bursts of 3 pulses at 50Hz were delivered in 2 second trains (5Hz) with an 8 second inter-train interval. Stimulation sessions were delivered hourly. Ten sessions were applied per day (18,000 pulses/day) for five consecutive days (90,000 pulses in total). Stimulation was delivered at 90% resting motor threshold (rMT). A depth correction (Stokes et al., 2005) was applied to the resting motor threshold to adjust for differences in the cortical depth of the individual's functional target compared to the primary motor cortex in order to consistently achieve 90% rMT in the intended functional target, but stimulation was never delivered above 120% rMT for safety. A Localite Neuronavigation System (Localite GmbH, Sankt Augustin, Germany) was used to position the TMS coil over the individualized functional stimulation target. All participants in this report's subset completed the full five-day treatment course.

Clinical assessment

Participants' depressive symptoms were assessed using the Hamilton Depression Rating Scale-17 item (HAMD-17) (Hamilton, 1960) and Montgomery-Asberg Depression Rating Scale (MADRS) (Montgomery and Asberg, 1979). HAMD-17 and MADRS assessments were performed one day before SAINT (baseline) and one day after the five-day SAINT treatment (post-treatment).

MRI image data acquisition and preprocessing

All participants were screened for MRI safety prior to any scanning procedures. MRI scans were acquired one day before SAINT (baseline) and one day after the five-day SAINT treatment (post-treatment). Each participant underwent identical baseline and post-treatment MRI scans consisting of structural and resting-state functional MRI acquisitions. All MRI scans were acquired using a 3T GE Discovery MR750 scanner with a 32-channel head-neck imaging coil at the Center for Cognitive and Neurobiological Imaging at Stanford.

High-resolution structural images using GE's "BRAVO" sequence (three-dimensional, T1-weighted) were acquired for the whole brain (FOV=256x256mm; matrix=256x256 voxel; slice thickness=0.9mm; TR=2530ms, TE=2.98ms, flip angle=7°).

The resting state scan consisted of a single 8-minute eyes-open resting scan. During resting state scans, participants were instructed to keep their eyes open and their attention focused on a central fixation point, which consisted of a black screen with a white fixation cross. Participants were also instructed to let their minds wander freely and to avoid any repetitive thoughts such as counting. Whole-brain resting-state scans were collected with a 3X simultaneous multi-slice (i.e. multiband) acquisition echo planar imaging (EPI) sequence: TR=2000ms, TE=30ms, flip angle=77°, slice acceleration factor=3, FOV=230x230mm, matrix=128×128 voxel, 1.8×1.8 mm^2 in-plane resolution, 87 contiguous axial slices parallel to the anterior commissure - posterior commissure line, yielding >1.4M voxels every 2 seconds. Head motion of participants was effectively minimized with the use of memory foam and inflatable padding. Participant alertness during the resting state task was monitored using in-scanner video cameras.

The MRI data were preprocessed using FMRIPREPR version 1.2.3 (Esteban et al., 2019) [RRID:SCR_016216]. Each T1-weighted volume was corrected for intensity non-uniformity with N4BiasFieldCorrectionv2.1.0 (Tustison et al., 2010) and skull-stripped using antsBrainExtraction.shv2.1.0 (using the OASIS template). Spatial normalization to the ICBM 152 Nonlinear Asymmetrical template version 2009c (Fonov et al., 2009)[RRID:SCR_008796] was performed through nonlinear registration with the antsRegistration tool of ANTs v2.1.0 (Avants et al., 2008) [RRID:SCR_004757], using brain-extracted versions of both T1-weighted volume and template. Brain tissue segmentation of cerebrospinal fluid, white matter, and gray matter, was performed on the brain-extracted T1-weighted volume using fast (Zhang et al., 2001) (FSL v5.0.9, RRID:SCR_002823).

The resting state data were motion corrected and then transformed into standard space (MNI). Physiological noise regressors were extracted applying CompCor (Behzadi et al., 2007). Framewise displacement (Power et al., 2014) was calculated using the implementation of Nipype. Unsteady state volumes detected by FMRIPREPR were censored out (range 3 ~ 9, mean= 5.12, SD=1.15). ICA-based Automatic Removal Of Motion Artifacts was used to non-aggressively denoise the data (Pruim et al., 2015). Next nuisance signal regression was applied with signals from white matter and cerebrospinal fluid. All the volumes with framewise displacement (FD) greater than 0.2mm were excluded; this resulted in exclusion of one participant, as greater than half of the dataset had FD>0.2mm. All the data were spatially smoothed (6-mm-full-width, half-maximal Gaussian kernel) and temporal bandpass filtered (0.1-0.01 Hz).

Regions of interest (ROI)

For this initial analysis, we restricted our ROIs to brain regions that have consistently been reported to play a role in MDD and emotion regulation: DLPFC, VLPFC, DMN, sgACC, SN, insula, amygdala and striatum.

In line with prior studies (Fox et al., 2012a; Hamani et al., 2011; Li et al., 2010; Liston et al., 2014; Siegle et al., 2012), the DLPFC (BA9, BA46), VLPFC (BA44, BA45, BA47), and the sgACC (BA 25) were defined by Brodmann areas (BA), using the Talairach atlas (Lancaster et al., 2000). The four nodes of DMN were extracted from the Multi-Subject Dictionary Learning (MSDL) atlas. DMN nodes were labeled using MSDL nomenclature: fDMN (Frontal DMN: medial prefrontal cortex), mDMN (median DMN: posterior cingulate cortex and precuneus), lDMN (left DMN: left angular gyrus), rDMN (right DMN: right angular gyrus) (Varoquaux et al., 2011). The two nodes of the SN, including anterior insula (AI) and dorsal anterior cingulate cortex (dACC), and insula were also obtained from MSDL. The striatum and amygdala are large nuclei with heterogeneous functions (Avissar et al., 2017; Ball et al., 2007; Fareri et al., 2015; Fullana et al., 2017; Qin et al., 2014; Tziortzi et al., 2014); hence, we constructed our ROIs of these structures by subregions. The executive and limbic subregions of striatum were defined using Oxford-GSK-Imanova Striatal Connectivity Atlas (striatum-con-label-thr25-3sub) (Tziortzi et al., 2014). Amygdala and its subregions were extracted using the Julich histological atlas: centromedian amygdala (CMA), basolateral amygdala (BA), and superficial amygdala (SA) (Eickhoff et al., 2007).

Data analysis

All statistical analyses were conducted with R (R Core Team, 2016). Fc was calculated as the correlation (Pearson) of the activity pattern across time between ROIs. All Pearson correlation coefficients were then transformed into Fisher's Z score for further analysis. Changes in mean MADRS, HAMD-17, and fc were assessed with paired t-tests. Changes in MADRS and fc were expressed as percent change from baseline: Delta = 100*(post-treatment - baseline)/baseline; thus, negative values of MADRS changes indicate improvement in depression symptoms. Linear regression models were used to test the relationship between fc and depression scores. Statistical significance was corrected for multiple comparisons across all comparisons using false discovery rate (FDR, threshold q=0.05).

Results

Depression symptoms

We found similar changes in depression symptoms with SAINT in the subset of participants with a diagnosis of MDD and complete MRI datasets. Mean HAMD-17 significantly decreased from 26.280 (±4.909,

range 20-35) at baseline to 4.722 (±4.599, range 0-16) after treatment ($t_{(17)}$=11.275, p<.001). Mean MADRS significantly decreased from 33.220 (±5.208, range 27-44) at baseline to 4.833 (±5.813, range 0-19) after treatment ($t_{(17)}$=14.915, p<.001). Baseline HAMD-17 and MADRS scores were highly correlated (r=.817, p<.001), as were the percent-change scores from baseline to post-treatment (r=.948, p<.001). MADRS was used as the primary clinical outcome for all fc analyses, and all results are equivalent for HAMD-17.

Functional connectivity changes

We examined fc changes that occurred with SAINT. Paired t-tests (FDR-corrected) demonstrated significant decrease in fc between lsgACC and three of four DMN nodes (lsgACC-fDMN: $t_{(17)}$=2.335, q =.036; lsgACC-mDMN: $t_{(17)}$=3.027, q=.008; lsgACC-rDMN: $t_{(17)}$=2.660, q=.017). A similar trend was found for fc between lsgACC and lDMN ($t_{(17)}$=2.106, q=.06) (Figure 1).

Fc reductions were also observed between rDLPFC and amygdala ($t_{(17)}$=2.303, q=.036), and striatum (rDLPFC-limS: $t_{(17)}$=2.354, q=.032), between SN nodes and amygdala (AI-lCMA: $t_{(17)}$=3.601, q=.002; AI-rCMA: $t_{(17)}$=3.167, q=.006; dACC-rBA: $t_{(17)}$=2.515, q=.023; AI-rBA: $t_{(17)}$=2.206, q=.045), between DMN and amygdala (fDMN-rCMA: $t_{(17)}$=2.491, q=.024; fDMN-rSA: $t_{(17)}$=2.520, q=.023), between DMN and striatum (fDMN-limbic striatum: $t_{(17)}$=2.281, q=.039; rDMN-executive striatum: $t_{(17)}$=2.303, q=.037; rDMN-limbic striatum: $t_{(17)}$=2.279, q=.039), between left insula and amygdala (linsula-lCMA: $t_{(17)}$=2.177, q=.049, linsula-rBA: $t_{(17)}$=2.221, q=.045), between amygdala and striatum (lCMA-limbic striatum: $t_{(17)}$=2.515, q=.023), and between amygdala sub-regions (lCMA-rCMA: $t_{(17)}$=3.601, q=.002; lCMA-rBA: $t_{(17)}$=2.276, q=.024; rCMA-rSA: $t_{(17)}$=2.481, q=.040) (figure 1).

Functional connectivity changes associated with clinical changes

We assessed the relationship between changes (percent change from baseline) in fc and depression symptoms using standard linear regression techniques adjusted for multiple comparisons (FDR).

Changes in fc between lDLPFC and other ROIs were significantly associated with changes in MADRS scores with better clinical outcomes correlated with greater decreases in fc between lDLPFC and lCMA (R^2=.21, $t_{(17)}$=2.351; q=.033) and between lDLPFC and linsula (R^2=.228, $t_{(17)}$=2.452; q=.026). Similarly, changes in fc between insula and amygdala were significantly associated with changes in MADRS scores with better clinical outcomes correlated with greater decreases in fc between rinsula and rBA (R^2 = .215, $t_{(17)}$ = 2.377; q = .031). (figure 2).

In contrast, smaller magnitude reductions (and larger magnitude increases) in fc between sgACC and DMN nodes were associated with better clinical outcomes. Specifically, greater depression symptom improvements were correlated with increased fc between rsgACC and lDMN (R^2=.225, $t_{(17)}$=-2.437, q=.027)

and fc between lsgACC and mDMN (R^2=.219, $t_{(17)}$=-2.399, q=.029). Although the overall group mean fc decreased with SAINT (see prior section), larger magnitude percent-reductions in MADRS scores were associated with smaller reductions, or larger increases, in fc between sgACC and DMN. The same relationship was found for fc between linsula and rSA (R^2=.291, $t_{(17)}$=-2.827, q=.012). (Figure 2)

Gender and age were not found to be confounders (all p's > .05), and all significant effects remained when including gender and age as covariates in multiple-regression models (all q's < .05).

Baseline functional connectivity association with clinical changes

We assessed the association between baseline fc and changes in MADRS scores with a similar linear regression approach. Larger improvements in MADRS scores were correlated with lower baseline fc between lDMN and frontal cortex (rVLPFC-lDMN: R^2=.235, $t_{(17)}$=2.496; q=.024; rDLPFC-lDMN: R^2=.231, $t_{(17)}$=2.47; q=.026) and between lDMN and striatum (limbic striatum-lDMN: R^2=.312, $t_{(17)}$=2.951; q=.009; executive striatum-lDMN: R^2 = .306, $t_{(17)}$ = 2.917; q = .01). (Figure 3).

Gender and age were not found to be confounders (all p's > .05), and all significant effects remained when including gender and age as covariates in multiple-regression models (all q's < .05).

Comprehensive results

Please see Figure S1 for heat maps depicting all fc changes that were observed following SAINT. Please see Tables S2 to S4 for a comprehensive list of all results when analyses were limited to the subset of 16 participants who responded to SAINT and were remitted from their depressive episode at the end of treatment.

Discussion

The advent of SAINT has provided us with a unique opportunity to assess the fc changes that occur during rapid remission from severe, treatment-resistant MDD. The analysis we undertook in this initial report focused on brain regions associated with emotion regulation, and we found that fc significantly decreases between several of these regions following SAINT-induced remission from MDD, with the magnitude of fc change often correlating with symptom improvement. Moreover, we found pre-treatment connectivity between several regions to be predictive of the magnitude of this improvement.

Overall, our results highlight the important role of brain regions involved in regulation of emotion in the pathophysiology and treatment of MDD. Indeed, this conclusion can be traced to some of the earliest neuroimaging studies in the field of psychiatry, which reported observations of hypometabolism and

hypoperfusion in the lDLPFC of patients with MDD (Baxter et al., 1989; Drevets et al., 1997; Martinot et al., 1990). Later investigators would demonstrate that lDLPFC activity is restored with treatment of MDD (Brody et al., 2001; Kito et al., 2008; Koenigs and Grafman, 2009; Loo et al., 2003; Mayberg et al., 2000, 1999; Nahas et al., 2001; Speer et al., 2000), and this early data prompted investigators to begin hypothesizing a major role of top-down dysfunction in the pathophysiology of depression (Goodwin, 1997; Mayberg, 1997).

Similarly, concomitant increases in activity in sgACC have long been observed in patients during depressive episodes (George et al., 1993), and this has been hypothesized to be causally related to reductions in lDLPFC activity (Ito et al., 1996). This hypothesis has been reinforced by observations that antidepressant treatments lead to reductions in sgACC activity (Dougherty et al., 2003; Drevets et al., 2008; Goldapple et al., 2004; Koenigs and Grafman, 2009; Mayberg et al., 2005, 2000; Mottaghy et al., 2002; Nobler et al., 2001). For review, see Hamani et al (2011). This led to the conception of depression as dysregulation in corticolimbic systems (Mayberg, 1997). In recent years, this conception has continued to evolve to include neural networks and their interactions. Several groups have reported evidence that depression is associated with increased fc between sgACC and DMN (Berman et al., 2011; Chai et al., 2016; Greicius et al., 2007; Hamilton et al., 2015, 2011; Kaiser et al., 2016; Philippi et al., 2015; Zhu et al., 2012), and others have shown that stimulation of lDLPFC potentiates upstream neural circuits to normalize sgACC-DMN connectivity (Baeken et al., 2017, 2014; Liston et al., 2014; Philip et al., 2018a, 2018b). This does not seem to be limited to individuals with depression, as rTMS of lDLPFC also has been shown to improve mood and reduce connectivity between sgACC and DMN in never-depressed participants (Singh et al., 2019).

Consistent with these studies, our research demonstrated a significant reduction in mean sgACC-DMN connectivity after SAINT. Moreover, we observed significant reduction in fc between sgACC and three of four DMN nodes, with a nearly significant trend in the remaining node. The hyper activity/connectivity within DMN has been considered as evidence of dysfunction of rumination and self-referential processing, and treatment is hypothesized to normalize DMN activity/connectivity (Baeken et al., 2017, 2014; Liston et al., 2014; Philip et al., 2018a, 2018b). Our results here support this hypothesis and raise another important question: Does the magnitude of overall suppression of DMN fc track with antidepressant treatment efficacy? Prior studies have reported significant reductions in fc between sgACC and one to two nodes of DMN (Baeken et al., 2017, 2014; Liston et al., 2014; Philip et al., 2018a, 2018b); whereas, we observed significant reduction in fc in nearly all DMN nodes. Bearing in mind that SAINT induced remission in 90% of participants in a mean in 1-5 days (Cole et al., 2019), this question deserves careful consideration in future studies.

Interestingly, although across our group of participants fc between sgACC and DMN significantly decreased following SAINT, individual changes in fc magnitude showed that participants with the lowest

magnitude reductions in fc between sgACC and mDMN actually had the best clinical improvements (we did not observe significant correlations for the other DMN nodes). It is unclear how to interpret this. It could be that "normalization of fc between sgACC and DMN" contains more complexity than magnitude of fc change between 2 nodes, or that the heterogeneity in disease process leads to changes in fc that are challenging to predict at the individual level with current approaches. Others have reported the opposite direction of association with the largest improvements in depression being associated with the largest reductions in fc between sgACC and mDMN (Philip et al., 2018b); however, this set of patients had comorbid post-traumatic stress disorder, which may respond differently to rTMS of the lDLPFC (Yesavage et al., 2018). Further, both Philip et al. (2018b) and our current report found an overall reduction in mean fc between sgACC and DMN in participants with improved depressive symptoms. This possible discrepancy could also be due to the limited variability in post-treatment MADRS scores in our sample, and only one of four DMN nodes showed an association between sgACC fc and MADRS score changes. Thus, additional analyses of other and future studies will be crucial to determine the validity, reliability, and meaning of this association.

Our assessment of the association between baseline fc and clinical improvements in depression scores also revealed a central role of the DMN. Greater clinical improvements were associated with lower baseline fc between DMN and DLPFC, striatum, and ventrolateral prefrontal cortex. Although fc between DLPFC and DMN predicts efficacy of ECT (Moreno-Ortega et al., 2019), other studies with similar findings could not be located. Past studies that use fc to predict response have found that fc between stimulation site lDLPFC and striatum predicts TMS (Avissar et al., 2017; Du et al., 2018), and several groups have reported that fc between stimulation site and sgACC that is more negative results in greater reductions in depressive symptoms with rTMS (Cash et al., 2019; Fox et al., 2012b; Weigand et al., 2018). In our current study, we optimized targeting by stimulating the portion of lDLPFC with maximum anticorrelation with sgACC; thus, it is possible that this may underlie the striking reductions in depression symptoms we observed.

In addition to reduced fc between sgACC and DMN, we observed several changes in fc that suggest augmentation of emotional regulation. Specifically, we found reductions in connectivity between DLPFC and amygdala, insula, and limbic striatum to be associated with clinical improvement in depression. For rDLPFC-left amygdala fc, in addition to finding reduced positive fc, we also found that greater clinical improvement was associated with larger decreases in fc. Several fMRI studies have demonstrated that individuals with MDD have altered frontal connectivity with amygdala (Almeida et al., 2009; Beauregard et al., 2006; Erk et al., 2010; Greening et al., 2014; Stephanou et al., 2017). Depressed individuals may have increased positive connectivity between rDLPFC and left amygdala (Han et al., 2015; Liu et al., 2018), and individuals with depression have an impaired ability to regulate negative emotions (Beauregard et al., 2006).

Considering that non-depressed individuals can better suppress amygdala activity (Greening et al., 2014; Stephanou et al., 2017), our results here could represent a partial normalization of connectivity related to improved emotion regulation, i.e. baseline positive fc between rDLPFC-amygdala is pathological, a reduction in positive fc is improved, and negative fc is normalized; however, our experimental design did not include never-depressed participants, so this remains speculative. Our combined findings of changes in fc with sgACC and amygdala following DLPFC stimulation with SAINT is supported by recent work with interwoven TMS and fMRI that showed DLPFC stimulation engages these nodes (Oathes et al., 2018).

Similarly, we found that greater clinical improvements were associated with larger decreases in fc between lDLPFC and insula. Insula has a well-known role in interoception (Critchley et al., 2004; Zaki et al., 2012), and insula activity is correlated with abnormal interoception in MDD (Avery et al., 2014). Insula metabolism has been linked to predicting antidepressant treatment response, and has thus been proposed as a depression biomarker (McGrath et al., 2013). Our results here are similar to other reports. Theta-burst rTMS stimulation of lDLPFC has been reported to reduce the magnitude of fc between lDLPFC and r-insula (Iwabuchi et al., 2017) with baseline fc between these structures predicting clinical response (Iwabuchi et al., 2019). Interestingly, individuals with subthreshold depression have lower fc between DLPFC (laterality not specified) and l-insula compared to non-depressed individuals (Hwang et al., 2015). This apparent directional mismatch highlights the importance of determining the causality of mechanism using within-subject analyses prior to using these findings as biomarkers to optimise treatment efficacy.

We also observed reduced fc in rDLPFC-limbic striatum following SAINT. Increased rDLPFC-dorsal caudate connectivity has been reported to correlate with increased depression severity (Kerestes et al., 2015), and fc between rDLPFC and ventral rostral putamen has been shown to decrease following depression treatment (Wang et al., 2017). Similarly, Furman et al found that depressed individuals have greater fc between DLPFC and dorsal caudate, and this fc was significantly correlated with depression severity, but they did not specify laterality (2011). This association has also been reported for lDLPFC-ventral striatum fc. Avissar et al reported that improvement in depression correlated with more reduction in lDLPFC-ventral striatum fc following treatment with rTMS of lDLPFC (Avissar et al., 2017). Thus, reducing DLPFC-striatum fc may be an important route to inducing remission from depression. The combined results show consistent association between significant changes in DLPFC fc with limbic structures following SAINT, which supports the hypothesis that regulation of emotion plays a central role in MDD.

This hypothesis is further supported by our observation that following SAINT we observed a significant decoupling of SN nodes, i.e. reduced fc between amygdala-insula, amygdala-dACC, amygdala-limbic striatum, and between amygdala subregions. Increased SN fc has been reported to be associated with decreased

anticipated pleasure (Rzepa and McCabe, 2016) and MDD (Manoliu et al., 2013). Further, other groups have reported that individuals with MDD have greater fc between insula and amygdala (Avery et al., 2014; Jacobs et al., 2016) and amygdala and striatum (Jacobs et al., 2016). This dysfunction in SN fc may underlie the biased reactivity to negative emotions observed in individuals with MDD (Manoliu et al., 2013; Strigo et al., 2008).

Some results we observed are more challenging to interpret. For example, we also observed that following SAINT fc significantly decreased between fDMN and multiple subregions of right amygdala and between multiple DMN nodes and striatum. rTMS of the lDLPFC has been shown to reduce fc between DMN and striatum in non-depressed individuals (Singh et al., 2019). However, other reports suggest the opposite association for mDMN (posterior cingulate cortex and precuneus): Individuals with depression have reduced fc between amygdala and precuneus compared to non-depressed controls (Wang et al., 2016), and connectivity between amygdala and posterior cingulate cortex is greater in less depressed individuals (Zhang et al., 2019). Our finding that fc between DMN and striatum decreased after SAINT is consistent with groups who have observed a similar change with antidepressant (Wang et al., 2019) and ECT treatment (Leaver et al., 2016). Others have reported that fc between mDMN and caudate is reduced in depressed individuals (Bluhm et al., 2009), indicating this may be a compensatory mechanism; however, this is complicated by reports that reduced fc between DMN and ventral striatum is associated with impaired reward responsivity (Sharma et al., 2017). Thus, a causal association between these changes in fc with depression is difficult to infer at this time.

Our observations should be considered in the context of the study's weaknesses. Foremost, the open-label design without a sham or standard-of-care rTMS control group limits our ability to determine if fc changes were due to SAINT, remission from MDD, or the passage of time. Sham-controlled, double-blinded assessment of SAINT is currently underway to address this important question. A strength and weakness of our analysis is the low variability in treatment-associated changes in depressive symptoms. Ninety percent of individuals were in remission from MDD following SAINT, with only two participants not remitting in this cohort, making statistical comparisons between remitters and non-remitters non-informative. Additionally, our linear-regression assessments demonstrated floor-effects, likely eliminating the potential to observe possible associations between changes in fc and clinical response. The small sample size further limited our likelihood of observing inter-individual differences. On the other hand, the high proportion of remitters increases our confidence in mean changes in functional connectivities across the group. Follow-up controlled trials will be helpful in determining the reliability of the findings we observed here. A limitation of our neuroimaging methods is that our resolution was insufficient to explore the role of hippocampus and its sub-regions. As the hippocampus has numerous reports describing an important role in depression (Liu et al., 2017), future studies of SAINT would benefit from assessment of fc related to this important structure. Finally, we included ROIs with

multiple prior reports demonstrating a role in emotion regulation; however, we did not confirm that the changes in fc that we observed were associated with changes in emotion regulation beyond standardized depression scales.

Depression remains a major public health problem with current treatments taking weeks to months to induce remission, and there are millions of people who are not effectively treated with current methods. Development of improved treatments could be accelerated by a better understanding of the neural changes that are necessary and sufficient to achieve disease remission. Our recent development of SAINT, which produces rapid and high rates of remission from MDD, provides an opportunity to begin searching for these neural changes. Our initial analysis of brain regions associated with emotion regulation demonstrates MDD remission is associated with a significant reduction in fc between sgACC and almost all major nodes of the DMN, bolstering prior hypotheses of the central role this network plays in MDD. We also found that decoupling of SN nodes was correlated with depression improvement, highlighting the role of other networks as well. Overall our results reinforce the hypothesis that emotional dysregulation is a central mechanism of MDD and treating emotional dysregulation is an effective treatment strategy. As our current study is based on an open-label trial of SAINT, controlled trials will be necessary to determine which observed changes in fc are unique to SAINT and disease remission in order to prioritize network-level targets for further treatment optimization.

References:

Almeida, J.R.C. de, Versace, A., Mechelli, A., Hassel, S., Quevedo, K., Kupfer, D.J., Phillips, M.L., 2009. Abnormal Amygdala-Prefrontal Effective Connectivity to Happy Faces Differentiates Bipolar from Major Depression. Biol. Psychiatry 66, 451–459. https://doi.org/10.1016/j.biopsych.2009.03.024

Avants, B., Epstein, C., Grossman, M., Gee, J., 2008. Symmetric diffeomorphic image registration with cross-correlation: Evaluating automated labeling of elderly and neurodegenerative brain. Med. Image Anal. 12, 26–41. https://doi.org/10.1016/j.media.2007.06.004

Avery, J.A., Drevets, W.C., Moseman, S.E., Bodurka, J., Barcalow, J.C., Simmons, W.K., 2014. Major Depressive Disorder Is Associated With Abnormal Interoceptive Activity and Functional Connectivity in the Insula. Biol. Psychiatry 76, 258–266. https://doi.org/10.1016/j.biopsych.2013.11.027

Avissar, M., Powell, F., Ilieva, I., Respino, M., Gunning, F.M., Liston, C., Dubin, M.J., 2017. Functional connectivity of the left DLPFC to striatum predicts treatment response of depression to TMS. Brain Stimulat. 10, 919–925. https://doi.org/10.1016/j.brs.2017.07.002

Baeken, C., Duprat, R., Wu, G.-R., De Raedt, R., van Heeringen, K., 2017. Subgenual Anterior Cingulate–Medial Orbitofrontal Functional Connectivity in Medication-Resistant Major Depression: A Neurobiological Marker for Accelerated Intermittent Theta Burst Stimulation Treatment? Biol. Psychiatry Cogn. Neurosci. Neuroimaging 2, 556–565. https://doi.org/10.1016/j.bpsc.2017.01.001

Baeken, C., Marinazzo, D., Wu, G.-R., Van Schuerbeek, P., De Mey, J., Marchetti, I., Vanderhasselt, M.-A., Remue, J., Luypaert, R., De Raedt, R., 2014. Accelerated HF-rTMS in treatment-resistant unipolar depression: Insights from subgenual anterior cingulate functional connectivity. World J. Biol. Psychiatry Off. J. World Fed. Soc. Biol. Psychiatry 15, 286–297. https://doi.org/10.3109/15622975.2013.872295

Ball, T., Rahm, B., Eickhoff, S.B., Schulze-Bonhage, A., Speck, O., Mutschler, I., 2007. Response Properties of Human Amygdala Subregions: Evidence Based on Functional MRI Combined with Probabilistic Anatomical Maps. PLoS ONE 2, e307. https://doi.org/10.1371/journal.pone.0000307

Baxter, L.R., Schwartz, J.M., Phelps, M.E., Mazziotta, J.C., Guze, B.H., Selin, C.E., Gerner, R.H., Sumida, R.M., 1989. Reduction of prefrontal cortex glucose metabolism common to three types of depression. Arch. Gen. Psychiatry 46, 243–250.

Beauregard, M., Paquette, V., Lévesque, J., 2006. Dysfunction in the neural circuitry of emotional self-regulation in major depressive disorder. Neuroreport 17, 843–846. https://doi.org/10.1097/01.wnr.0000220132.32091.9f

Behzadi, Y., Restom, K., Liau, J., Liu, T.T., 2007. A component based noise correction method (CompCor) for BOLD and perfusion based fMRI. NeuroImage 37, 90–101. https://doi.org/10.1016/j.neuroimage.2007.04.042

Berman, M.G., Peltier, S., Nee, D.E., Kross, E., Deldin, P.J., Jonides, J., 2011. Depression, rumination and the default network. Soc. Cogn. Affect. Neurosci. 6, 548–555. https://doi.org/10.1093/scan/nsq080

Bluhm, R., Williamson, P., Lanius, R., Théberge, J., Densmore, M., Bartha, R., Neufeld, R., Osuch, E., 2009. Resting state default-mode network connectivity in early depression using a seed region-of-interest analysis: decreased connectivity with caudate nucleus. Psychiatry Clin. Neurosci. 63, 754–761. https://doi.org/10.1111/j.1440-1819.2009.02030.x

Brody, A.L., Saxena, S., Mandelkern, M.A., Fairbanks, L.A., Ho, M.L., Baxter, L.R., 2001. Brain metabolic changes associated with symptom factor improvement in major depressive disorder. Biol. Psychiatry 50, 171–178.

Cash, R.F.H., Zalesky, A., Thomson, R.H., Tian, Y., Cocchi, L., Fitzgerald, P.B., 2019. Subgenual functional connectivity predicts antidepressant treatment response to transcranial magnetic stimulation: independent validation and evaluation of personalization. Biol. Psychiatry.

https://doi.org/10.1016/j.biopsych.2018.12.002
Chai, X.J., Hirshfeld-Becker, D., Biederman, J., Uchida, M., Doehrmann, O., Leonard, J.A., Salvatore, J., Kenworthy, T., Brown, A., Kagan, E., de los Angeles, C., Gabrieli, J.D.E., Whitfield-Gabrieli, S., 2016. Altered Intrinsic Functional Brain Architecture in Children at Familial Risk of Major Depression. Biol. Psychiatry 80, 849–858. https://doi.org/10.1016/j.biopsych.2015.12.003
Chen, A.C., Oathes, D.J., Chang, C., Bradley, T., Zhou, Z.-W., Williams, L.M., Glover, G.H., Deisseroth, K., Etkin, A., 2013. Causal interactions between fronto-parietal central executive and default-mode networks in humans. Proc. Natl. Acad. Sci. 110, 19944–19949. https://doi.org/10.1073/pnas.1311772110
Cole, E.J., Stimpson, K.H., Bentzley, B.S., Gulser, M., Cherian, K., Tischler, C., Nejad, R., Pankow, H., Choi, E., Aaron, H., Espil, F.M., Pannu, J., Xiao, X., Duvio, D., Solvason, H.B., Hawkins, J., Guerra, A., Jo, B., Raj, K.S., Debattista, C., Keller, J., Schatzberg, A.F., Sudheimer, K.D., Williams, N.R., 2019. Stanford Accelerated Intelligent Neuromodulation Therapy for Treatment-Resistant Depression (SAINT-TRD). bioRxiv. https://doi.org/10.1101/581280
Connolly, C.G., Ho, T.C., Blom, E.H., LeWinn, K.Z., Sacchet, M.D., Tymofiyeva, O., Simmons, A.N., Yang, T.T., 2017. Resting-state functional connectivity of the amygdala and longitudinal changes in depression severity in adolescent depression. J. Affect. Disord. 207, 86–94. https://doi.org/10.1016/j.jad.2016.09.026
Critchley, H.D., Wiens, S., Rotshtein, P., Öhman, A., Dolan, R.J., 2004. Neural systems supporting interoceptive awareness. Nat. Neurosci. 7, 189–195. https://doi.org/10.1038/nn1176
de Kwaasteniet, B., Ruhe, E., Caan, M., Rive, M., Olabarriaga, S., Groefsema, M., Heesink, L., van Wingen, G., Denys, D., 2013. Relation between structural and functional connectivity in major depressive disorder. Biol. Psychiatry 74, 40–47. https://doi.org/10.1016/j.biopsych.2012.12.024
De Raedt, R., Leyman, L., Baeken, C., Van Schuerbeek, P., Luypaert, R., Vanderhasselt, M.-A., Dannlowski, U., 2010. Neurocognitive effects of HF-rTMS over the dorsolateral prefrontal cortex on the attentional processing of emotional information in healthy women: an event-related fMRI study. Biol. Psychol. 85, 487–495. https://doi.org/10.1016/j.biopsycho.2010.09.015
Dinga, R., Schmaal, L., Penninx, B., Tol, M.J. van, Veltman, D.J., Velzen, L. van, Wee, N. van der, Marquand, A., 2018. Evaluating the evidence for biotypes of depression: attempted replication of Drysdale et.al. 2017. bioRxiv 416321. https://doi.org/10.1101/416321
Dougherty, D.D., Weiss, A.P., Cosgrove, G.R., Alpert, N.M., Cassem, E.H., Nierenberg, A.A., Price, B.H., Mayberg, H.S., Fischman, A.J., Rauch, S.L., 2003. Cerebral metabolic correlates as potential predictors of response to anterior cingulotomy for treatment of major depression. J. Neurosurg. 99, 1010–1017. https://doi.org/10.3171/jns.2003.99.6.1010
Drevets, W.C., Price, J.L., Simpson, J.R., Todd, R.D., Reich, T., Vannier, M., Raichle, M.E., 1997. Subgenual prefrontal cortex abnormalities in mood disorders. Nature 386, 824–827. https://doi.org/10.1038/386824a0
Drevets, W.C., Savitz, J., Trimble, M., 2008. The Subgenual Anterior Cingulate Cortex in Mood Disorders. CNS Spectr. 13, 663–681.
Drysdale, A.T., Grosenick, L., Downar, J., Dunlop, K., Mansouri, F., Meng, Y., Fetcho, R.N., Zebley, B., Oathes, D.J., Etkin, A., Schatzberg, A.F., Sudheimer, K., Keller, J., Mayberg, H.S., Gunning, F.M., Alexopoulos, G.S., Fox, M.D., Pascual-Leone, A., Voss, H.U., Casey, B.J., Dubin, M.J., Liston, C., 2017. Resting-state connectivity biomarkers define neurophysiological subtypes of depression. Nat. Med. 23, 28–38. https://doi.org/10.1038/nm.4246
Du, L., Liu, H., Du, W., Chao, F., Zhang, L., Wang, K., Huang, C., Gao, Y., Tang, Y., 2018. Stimulated left DLPFC-nucleus accumbens functional connectivity predicts the anti-depression and anti-anxiety effects of rTMS for depression. Transl. Psychiatry 7, 3. https://doi.org/10.1038/s41398-017-0005-6

Eickhoff, S.B., Paus, T., Caspers, S., Grosbras, M.-H., Evans, A.C., Zilles, K., Amunts, K., 2007. Assignment of functional activations to probabilistic cytoarchitectonic areas revisited. NeuroImage 36, 511–521. https://doi.org/10.1016/j.neuroimage.2007.03.060

Erk, S., Mikschl, A., Stier, S., Ciaramidaro, A., Gapp, V., Weber, B., Walter, H., 2010. Acute and sustained effects of cognitive emotion regulation in major depression. J. Neurosci. Off. J. Soc. Neurosci. 30, 15726–15734. https://doi.org/10.1523/JNEUROSCI.1856-10.2010

Esteban, O., Markiewicz, C.J., Blair, R.W., Moodie, C.A., Isik, A.I., Erramuzpe, A., Kent, J.D., Goncalves, M., DuPre, E., Snyder, M., Oya, H., Ghosh, S.S., Wright, J., Durnez, J., Poldrack, R.A., Gorgolewski, K.J., 2019. fMRIPrep: a robust preprocessing pipeline for functional MRI. Nat. Methods 16, 111–116. https://doi.org/10.1038/s41592-018-0235-4

Etkin, A., Büchel, C., Gross, J.J., 2015. The neural bases of emotion regulation. Nat. Rev. Neurosci. 16, 693–700. https://doi.org/10.1038/nrn4044

Fareri, D.S., Gabard-Durnam, L., Goff, B., Flannery, J., Gee, D.G., Lumian, D.S., Caldera, C., Tottenham, N., 2015. Normative development of ventral striatal resting state connectivity in humans. NeuroImage 118, 422–437. https://doi.org/10.1016/j.neuroimage.2015.06.022

Fischer, A.S., Keller, C.J., Etkin, A., 2016. The Clinical Applicability of Functional Connectivity in Depression: Pathways Toward More Targeted Intervention. Biol. Psychiatry Cogn. Neurosci. Neuroimaging 1, 262–270. https://doi.org/10.1016/j.bpsc.2016.02.004

Fonov, V., Evans, A., McKinstry, R., Almli, C., Collins, D., 2009. Unbiased nonlinear average age-appropriate brain templates from birth to adulthood. NeuroImage 47, S102. https://doi.org/10.1016/S1053-8119(09)70884-5

Fox, M.D., Buckner, R.L., White, M.P., Greicius, M.D., Pascual-Leone, A., 2012a. Efficacy of transcranial magnetic stimulation targets for depression is related to intrinsic functional connectivity with the subgenual cingulate. Biol. Psychiatry 72, 595–603. https://doi.org/10.1016/j.biopsych.2012.04.028

Fox, M.D., Halko, M.A., Eldaief, M.C., Pascual-Leone, A., 2012b. Measuring and manipulating brain connectivity with resting state functional connectivity magnetic resonance imaging (fcMRI) and transcranial magnetic stimulation (TMS). NeuroImage 62, 2232–2243. https://doi.org/10.1016/j.neuroimage.2012.03.035

Friedrich, M.J., 2017. Depression Is the Leading Cause of Disability Around the World. JAMA 317, 1517–1517. https://doi.org/10.1001/jama.2017.3826

Fullana, M.A., Zhu, X., Alonso, P., Cardoner, N., Real, E., López-Solà, C., Segalàs, C., Subirà, M., Galfalvy, H., Menchón, J.M., Simpson, H.B., Marsh, R., Soriano-Mas, C., 2017. Basolateral amygdala–ventromedial prefrontal cortex connectivity predicts cognitive behavioural therapy outcome in adults with obsessive–compulsive disorder. J. Psychiatry Neurosci. 42, 378–385. https://doi.org/10.1503/jpn.160215

Furman, D.J., Hamilton, J.P., Gotlib, I.H., 2011. Frontostriatal functional connectivity in major depressive disorder. Biol. Mood Anxiety Disord. 1, 11. https://doi.org/10.1186/2045-5380-1-11

George, M.S., Ketter, T.A., Post, R.M., 1993. SPECT and PET imaging in mood disorders. J. Clin. Psychiatry 54 Suppl, 6–13.

George, M.S., Lisanby, S.H., Avery, D., McDonald, W.M., Durkalski, V., Pavlicova, M., Anderson, B., Nahas, Z., Bulow, P., Zarkowski, P., Holtzheimer, P.E., Schwartz, T., Sackeim, H.A., 2010. Daily left prefrontal transcranial magnetic stimulation therapy for major depressive disorder: a sham-controlled randomized trial. Arch. Gen. Psychiatry 67, 507–516. https://doi.org/10.1001/archgenpsychiatry.2010.46

Goldapple, K., Segal, Z., Garson, C., Lau, M., Bieling, P., Kennedy, S., Mayberg, H., 2004. Modulation of cortical-limbic pathways in major depression: treatment-specific effects of cognitive behavior therapy. Arch. Gen. Psychiatry 61, 34–41. https://doi.org/10.1001/archpsyc.61.1.34

Goodwin, G.M., 1997. Neuropsychological and neuroimaging evidence for the involvement of the frontal lobes

in depression. J. Psychopharmacol. Oxf. Engl. 11, 115–122. https://doi.org/10.1177/026988119701100204
Greening, S.G., Osuch, E.A., Williamson, P.C., Mitchell, D.G.V., 2014. The neural correlates of regulating positive and negative emotions in medication-free major depression. Soc. Cogn. Affect. Neurosci. 9, 628–637. https://doi.org/10.1093/scan/nst027
Greicius, M.D., Flores, B.H., Menon, V., Glover, G.H., Solvason, H.B., Kenna, H., Reiss, A.L., Schatzberg, A.F., 2007. Resting-state functional connectivity in major depression: abnormally increased contributions from subgenual cingulate cortex and thalamus. Biol. Psychiatry 62, 429–437. https://doi.org/10.1016/j.biopsych.2006.09.020
Hamani, C., Mayberg, H., Stone, S., Laxton, A., Haber, S., Lozano, A.M., 2011. The subcallosal cingulate gyrus in the context of major depression. Biol. Psychiatry 69, 301–308. https://doi.org/10.1016/j.biopsych.2010.09.034
Hamilton, J.P., Farmer, M., Fogelman, P., Gotlib, I.H., 2015. Depressive Rumination, the Default-Mode Network, and the Dark Matter of Clinical Neuroscience. Biol. Psychiatry 78, 224–230. https://doi.org/10.1016/j.biopsych.2015.02.020
Hamilton, J.P., Furman, D.J., Chang, C., Thomason, M.E., Dennis, E., Gotlib, I.H., 2011. Default-mode and task-positive network activity in major depressive disorder: implications for adaptive and maladaptive rumination. Biol. Psychiatry 70, 327–333. https://doi.org/10.1016/j.biopsych.2011.02.003
Hamilton, M., 1960. A rating scale for depression. J. Neurol. Neurosurg. Psychiatry 23, 56–62.
Han, K., Chapman, S.B., Krawczyk, D.C., 2015. Altered Amygdala Connectivity in Individuals with Chronic Traumatic Brain Injury and Comorbid Depressive Symptoms. Front. Neurol. 6, 231. https://doi.org/10.3389/fneur.2015.00231
Hasin, D.S., Sarvet, A.L., Meyers, J.L., Saha, T.D., Ruan, W.J., Stohl, M., Grant, B.F., 2018. Epidemiology of Adult DSM-5 Major Depressive Disorder and Its Specifiers in the United States. JAMA Psychiatry 75, 336–346. https://doi.org/10.1001/jamapsychiatry.2017.4602
Heijnen, W.T., Birkenhäger, T.K., Wierdsma, A.I., van den Broek, W.W., 2010. Antidepressant pharmacotherapy failure and response to subsequent electroconvulsive therapy: a meta-analysis. J. Clin. Psychopharmacol. 30, 616–619. https://doi.org/10.1097/JCP.0b013e3181ee0f5f
Hwang, J.W., Egorova, N., Yang, X.Q., Zhang, W.Y., Chen, J., Yang, X.Y., Hu, L.J., Sun, S., Tu, Y., Kong, J., 2015. Subthreshold depression is associated with impaired resting-state functional connectivity of the cognitive control network. Transl. Psychiatry 5, e683. https://doi.org/10.1038/tp.2015.174
Ito, H., Kawashima, R., Awata, S., Ono, S., Sato, K., Goto, R., Koyama, M., Sato, M., Fukuda, H., 1996. Hypoperfusion in the limbic system and prefrontal cortex in depression: SPECT with anatomic standardization technique. J. Nucl. Med. Off. Publ. Soc. Nucl. Med. 37, 410–414.
Iwabuchi, S.J., Auer, D.P., Lankappa, S.T., Palaniyappan, L., 2019. Baseline effective connectivity predicts response to repetitive transcranial magnetic stimulation in patients with treatment-resistant depression. Eur. Neuropsychopharmacol. J. Eur. Coll. Neuropsychopharmacol. 29, 681–690. https://doi.org/10.1016/j.euroneuro.2019.02.012
Iwabuchi, S.J., Raschke, F., Auer, D.P., Liddle, P.F., Lankappa, S.T., Palaniyappan, L., 2017. Targeted transcranial theta-burst stimulation alters fronto-insular network and prefrontal GABA. NeuroImage 146, 395–403. https://doi.org/10.1016/j.neuroimage.2016.09.043
Jacobs, R.H., Barba, A., Gowins, J.R., Klumpp, H., Jenkins, L.M., Mickey, B.J., Ajilore, O., Peciña, M., Sikora, M., Ryan, K.A., Hsu, D.T., Welsh, R.C., Zubieta, J.-K., Phan, K.L., Langenecker, S.A., 2016. Decoupling of the amygdala to other salience network regions in adolescent-onset recurrent major depressive disorder. Psychol. Med. 46, 1055–1067. https://doi.org/10.1017/S0033291715002615
Joormann, J., Vanderlind, W.M., 2014. Emotion regulation in depression: The role of biased cognition and reduced cognitive control. Clin. Psychol. Sci. 2, 402–421.

Kaiser, R.H., Whitfield-Gabrieli, S., Dillon, D.G., Goer, F., Beltzer, M., Minkel, J., Smoski, M., Dichter, G., Pizzagalli, D.A., 2016. Dynamic Resting-State Functional Connectivity in Major Depression. Neuropsychopharmacol. Off. Publ. Am. Coll. Neuropsychopharmacol. 41, 1822–1830. https://doi.org/10.1038/npp.2015.352

Kerestes, R., Harrison, B.J., Dandash, O., Stephanou, K., Whittle, S., Pujol, J., Davey, C.G., 2015. Specific functional connectivity alterations of the dorsal striatum in young people with depression. NeuroImage Clin. 7, 266–272. https://doi.org/10.1016/j.nicl.2014.12.017

Kito, S., Fujita, K., Koga, Y., 2008. Regional Cerebral Blood Flow Changes after Low-Frequency Transcranial Magnetic Stimulation of the Right Dorsolateral Prefrontal Cortex in Treatment-Resistant Depression. Neuropsychobiology 58, 29–36. https://doi.org/10.1159/000154477

Koenigs, M., Grafman, J., 2009. The functional neuroanatomy of depression: distinct roles for ventromedial and dorsolateral prefrontal cortex. Behav. Brain Res. 201, 239–243. https://doi.org/10.1016/j.bbr.2009.03.004

Lantrip, C., Gunning, F.M., Flashman, L., Roth, R.M., Holtzheimer, P.E., 2017. Effects of Transcranial Magnetic Stimulation on the Cognitive Control of Emotion: Potential Antidepressant Mechanisms. J. ECT 33, 73–80. https://doi.org/10.1097/YCT.0000000000000386

Leaver, A.M., Espinoza, R., Joshi, S.H., Vasavada, M., Njau, S., Woods, R.P., Narr, K.L., 2016. Desynchronization and Plasticity of Striato-frontal Connectivity in Major Depressive Disorder. Cereb. Cortex N. Y. N 1991 26, 4337–4346. https://doi.org/10.1093/cercor/bhv207

Levkovitz, Y., Isserles, M., Padberg, F., Lisanby, S.H., Bystritsky, A., Xia, G., Tendler, A., Daskalakis, Z.J., Winston, J.L., Dannon, P., Hafez, H.M., Reti, I.M., Morales, O.G., Schlaepfer, T.E., Hollander, E., Berman, J.A., Husain, M.M., Sofer, U., Stein, A., Adler, S., Deutsch, L., Deutsch, F., Roth, Y., George, M.S., Zangen, A., 2015. Efficacy and safety of deep transcranial magnetic stimulation for major depression: a prospective multicenter randomized controlled trial. World Psychiatry 14, 64–73. https://doi.org/10.1002/wps.20199

Li, C.-T., Lin, C.-P., Chou, K.-H., Chen, I.-Y., Hsieh, J.-C., Wu, C.-L., Lin, W.-C., Su, T.-P., 2010. Structural and cognitive deficits in remitting and non-remitting recurrent depression: A voxel-based morphometric study. NeuroImage 50, 347–356. https://doi.org/10.1016/j.neuroimage.2009.11.021

Li, W., Ward, B.D., Xie, C., Jones, J.L., Antuono, P.G., Li, S.-J., Goveas, J.S., 2015. Amygdala network dysfunction in late-life depression phenotypes: Relationships with symptom dimensions. J. Psychiatr. Res. 70, 121–129. https://doi.org/10.1016/j.jpsychires.2015.09.002

Liston, C., Chen, A.C., Zebley, B.D., Drysdale, A.T., Gordon, R., Leuchter, B., Voss, H.U., Casey, B.J., Etkin, A., Dubin, M.J., 2014. Default Mode Network Mechanisms of Transcranial Magnetic Stimulation in Depression. Biol. Psychiatry 76, 517–526. https://doi.org/10.1016/j.biopsych.2014.01.023

Liu, L., Yao, Y.-W., Li, C.-S.R., Zhang, J.-T., Xia, C.-C., Lan, J., Ma, S.-S., Zhou, N., Fang, X.-Y., 2018. The Comorbidity Between Internet Gaming Disorder and Depression: Interrelationship and Neural Mechanisms. Front. Psychiatry 9, 154. https://doi.org/10.3389/fpsyt.2018.00154

Liu, W., Ge, T., Leng, Y., Pan, Z., Fan, J., Yang, W., Cui, R., 2017. The Role of Neural Plasticity in Depression: From Hippocampus to Prefrontal Cortex. Neural Plast. 2017, 6871089. https://doi.org/10.1155/2017/6871089

Loo, C.K., Sachdev, P.S., Haindl, W., Wen, W., Mitchell, P.B., Croker, V.M., Malhi, G.S., 2003. High (15 Hz) and low (1 Hz) frequency transcranial magnetic stimulation have different acute effects on regional cerebral blood flow in depressed patients. Psychol. Med. 33, 997–1006. https://doi.org/10.1017/S0033291703007955

Luber, B.M., Davis, S., Bernhardt, E., Neacsiu, A., Kwapil, L., Lisanby, S.H., Strauman, T.J., 2017. Using neuroimaging to individualize TMS treatment for depression: Toward a new paradigm for imaging-guided intervention. NeuroImage 148, 1–7. https://doi.org/10.1016/j.neuroimage.2016.12.083

Manoliu, A., Meng, C., Brandl, F., Doll, A., Tahmasian, M., Scherr, M., Schwerthöffer, D., Zimmer, C., Förstl, H., Bäuml, J., Riedl, V., Wohlschläger, A.M., Sorg, C., 2013. Insular dysfunction within the salience network is associated with severity of symptoms and aberrant inter-network connectivity in major depressive disorder. Front. Hum. Neurosci. 7, 930. https://doi.org/10.3389/fnhum.2013.00930

Martinot, J., Hardy, P., Feline, A., Huret, J., Mazoyer, B., Attar-Levy, D., Pappata, S., Syrota, A., 1990. Left prefrontal glucose hypometabolism in the depressed state: a confirmation. Am. J. Psychiatry 147, 1313–1317. https://doi.org/10.1176/ajp.147.10.1313

Mayberg, H.S., 1997. Limbic-cortical dysregulation: a proposed model of depression. J. Neuropsychiatry Clin. Neurosci. 9, 471–481.

Mayberg, H.S., Brannan, S.K., Tekell, J.L., Silva, J.A., Mahurin, R.K., McGinnis, S., Jerabek, P.A., 2000. Regional metabolic effects of fluoxetine in major depression: serial changes and relationship to clinical response. Biol. Psychiatry 48, 830–843.

Mayberg, H.S., Liotti, M., Brannan, S.K., McGinnis, S., Mahurin, R.K., Jerabek, P.A., Silva, J.A., Tekell, J.L., Martin, C.C., Lancaster, J.L., Fox, P.T., 1999. Reciprocal limbic-cortical function and negative mood: converging PET findings in depression and normal sadness. Am. J. Psychiatry 156, 675–682. https://doi.org/10.1176/ajp.156.5.675

Mayberg, H.S., Lozano, A.M., Voon, V., McNeely, H.E., Seminowicz, D., Hamani, C., Schwalb, J.M., Kennedy, S.H., 2005. Deep brain stimulation for treatment-resistant depression. Neuron 45, 651–660. https://doi.org/10.1016/j.neuron.2005.02.014

McGrath, C.L., Kelley, M.E., Holtzheimer, P.E., Dunlop, B.W., Craighead, W.E., Franco, A.R., Craddock, R.C., Mayberg, H.S., 2013. Toward a neuroimaging treatment selection biomarker for major depressive disorder. JAMA Psychiatry 70, 821–829. https://doi.org/10.1001/jamapsychiatry.2013.143

Moreno-Ortega, M., Prudic, J., Rowny, S., Patel, G.H., Kangarlu, A., Lee, S., Grinband, J., Palomo, T., Perera, T., Glasser, M.F., Javitt, D.C., 2019. Resting state functional connectivity predictors of treatment response to electroconvulsive therapy in depression. Sci. Rep. 9, 5071. https://doi.org/10.1038/s41598-019-41175-4

Mottaghy, F.M., Keller, C.E., Gangitano, M., Ly, J., Thall, M., Parker, J.A., Pascual-Leone, A., 2002. Correlation of cerebral blood flow and treatment effects of repetitive transcranial magnetic stimulation in depressed patients. Psychiatry Res. 115, 1–14.

Nahas, Z., Teneback, C.C., Kozel, A., Speer, A.M., DeBrux, C., Molloy, M., Stallings, L., Spicer, K.M., Arana, G., Bohning, D.E., Risch, S.C., George, M.S., 2001. Brain Effects of TMS Delivered Over Prefrontal Cortex in Depressed Adults: Role of Stimulation Frequency and Coil–Cortex Distance. J. Neuropsychiatry Clin. Neurosci. 13, 459–470. https://doi.org/10.1176/jnp.13.4.459

Nobler, M.S., Oquendo, M.A., Kegeles, L.S., Malone, K.M., Campbell, C.C., Sackeim, H.A., Mann, J.J., 2001. Decreased regional brain metabolism after ect. Am. J. Psychiatry 158, 305–308. https://doi.org/10.1176/appi.ajp.158.2.305

Oathes, D.J., Zimmerman, J., Duprat, R., Cavdaroglu, S., Scully, M., Rosenberg, B., Flounders, M.W., Long, H., Elliott, M., Shandler, G., Shinohara, R.T., Linn, K.A., 2018. Individualized non-invasive brain stimulation engages the subgenual anterior cingulate and amygdala. bioRxiv 503441. https://doi.org/10.1101/503441

O'Reardon, J.P., Solvason, H.B., Janicak, P.G., Sampson, S., Isenberg, K.E., Nahas, Z., McDonald, W.M., Avery, D., Fitzgerald, P.B., Loo, C., Demitrack, M.A., George, M.S., Sackeim, H.A., 2007. Efficacy and Safety of Transcranial Magnetic Stimulation in the Acute Treatment of Major Depression: A Multisite Randomized Controlled Trial. Biol. Psychiatry, Depression: New Perspectives on Treatment and Etiology 62, 1208–1216. https://doi.org/10.1016/j.biopsych.2007.01.018

Pan, P.M., Sato, J.R., Salum, G.A., Rohde, L.A., Gadelha, A., Zugman, A., Mari, J., Jackowski, A., Picon, F., Miguel, E.C., Pine, D.S., Leibenluft, E., Bressan, R.A., Stringaris, A., 2017. Ventral Striatum Functional

Connectivity as a Predictor of Adolescent Depressive Disorder in a Longitudinal Community-Based Sample. Am. J. Psychiatry 174, 1112–1119. https://doi.org/10.1176/appi.ajp.2017.17040430

Pannekoek, J.N., van der Werff, S.J.A., Meens, P.H.F., van den Bulk, B.G., Jolles, D.D., Veer, I.M., van Lang, N.D.J., Rombouts, S.A.R.B., van der Wee, N.J.A., Vermeiren, R.R.J.M., 2014. Aberrant resting-state functional connectivity in limbic and salience networks in treatment--naïve clinically depressed adolescents. J. Child Psychol. Psychiatry 55, 1317–1327. https://doi.org/10.1111/jcpp.12266

Peters, A.T., Burkhouse, K., Feldhaus, C.C., Langenecker, S.A., Jacobs, R.H., 2016. Aberrant resting-state functional connectivity in limbic and cognitive control networks relates to depressive rumination and mindfulness: A pilot study among adolescents with a history of depression. J. Affect. Disord. 200, 178–181. https://doi.org/10.1016/j.jad.2016.03.059

Philip, N.S., Barredo, J., Aiken, E., Carpenter, L.L., 2018a. Neuroimaging Mechanisms of Therapeutic Transcranial Magnetic Stimulation for Major Depressive Disorder. Biol. Psychiatry Cogn. Neurosci. Neuroimaging 3, 211–222. https://doi.org/10.1016/j.bpsc.2017.10.007

Philip, N.S., Barredo, J., van ’t Wout-Frank, M., Tyrka, A.R., Price, L.H., Carpenter, L.L., 2018b. Network Mechanisms of Clinical Response to Transcranial Magnetic Stimulation in Posttraumatic Stress Disorder and Major Depressive Disorder. Biol. Psychiatry 83, 263–272. https://doi.org/10.1016/j.biopsych.2017.07.021

Philippi, C.L., Motzkin, J.C., Pujara, M.S., Koenigs, M., 2015. Subclinical depression severity is associated with distinct patterns of functional connectivity for subregions of anterior cingulate cortex. J. Psychiatr. Res. 71, 103–111. https://doi.org/10.1016/j.jpsychires.2015.10.005

Power, J.D., Mitra, A., Laumann, T.O., Snyder, A.Z., Schlaggar, B.L., Petersen, S.E., 2014. Methods to detect, characterize, and remove motion artifact in resting state fMRI. NeuroImage 84, 320–341. https://doi.org/10.1016/j.neuroimage.2013.08.048

Pruim, R.H.R., Mennes, M., van Rooij, D., Llera, A., Buitelaar, J.K., Beckmann, C.F., 2015. ICA-AROMA: A robust ICA-based strategy for removing motion artifacts from fMRI data. NeuroImage 112, 267–277. https://doi.org/10.1016/j.neuroimage.2015.02.064

Qin, S., Young, C.B., Duan, X., Chen, T., Supekar, K., Menon, V., 2014. Amygdala Subregional Structure and Intrinsic Functional Connectivity Predicts Individual Differences in Anxiety During Early Childhood. Biol. Psychiatry 75, 892–900. https://doi.org/10.1016/j.biopsych.2013.10.006

R Core Team, 2016. R: A Language and Environment for Statistical Computing. R Foundation for Statistical Computing, Vienna, Austria.

Redlich, R., Dohm, K., Grotegerd, D., Opel, N., Zwitserlood, P., Heindel, W., Arolt, V., Kugel, H., Dannlowski, U., 2015. Reward Processing in Unipolar and Bipolar Depression: A Functional MRI Study. Neuropsychopharmacol. Off. Publ. Am. Coll. Neuropsychopharmacol. 40, 2623–2631. https://doi.org/10.1038/npp.2015.110

Rive, M.M., van Rooijen, G., Veltman, D.J., Phillips, M.L., Schene, A.H., Ruhé, H.G., 2013. Neural correlates of dysfunctional emotion regulation in major depressive disorder. A systematic review of neuroimaging studies. Neurosci. Biobehav. Rev. 37, 2529–2553. https://doi.org/10.1016/j.neubiorev.2013.07.018

Rush, A.J., Trivedi, M.H., Wisniewski, S.R., Nierenberg, A.A., Stewart, J.W., Warden, D., Niederehe, G., Thase, M.E., Lavori, P.W., Lebowitz, B.D., McGrath, P.J., Rosenbaum, J.F., Sackeim, H.A., Kupfer, D.J., Luther, J., Fava, M., 2006. Acute and longer-term outcomes in depressed outpatients requiring one or several treatment steps: a STAR*D report. Am. J. Psychiatry 163, 1905–1917. https://doi.org/10.1176/appi.ajp.163.11.1905

Rzepa, E., McCabe, C., 2016. Decreased anticipated pleasure correlates with increased salience network resting state functional connectivity in adolescents with depressive symptomatology. J. Psychiatr. Res. 82, 40–47. https://doi.org/10.1016/j.jpsychires.2016.07.013

Sharma, A., Wolf, D.H., Ciric, R., Kable, J.W., Moore, T.M., Vandekar, S.N., Katchmar, N., Daldal, A., Ruparel,

K., Davatzikos, C., Elliott, M.A., Calkins, M.E., Shinohara, R.T., Bassett, D.S., Satterthwaite, T.D., 2017. Common Dimensional Reward Deficits Across Mood and Psychotic Disorders: A Connectome-Wide Association Study. Am. J. Psychiatry 174, 657–666. https://doi.org/10.1176/appi.ajp.2016.16070774

Sheline, Y.I., Barch, D.M., Price, J.L., Rundle, M.M., Vaishnavi, S.N., Snyder, A.Z., Mintun, M.A., Wang, S., Coalson, R.S., Raichle, M.E., 2009. The default mode network and self-referential processes in depression. Proc. Natl. Acad. Sci. U. S. A. 106, 1942–1947. https://doi.org/10.1073/pnas.0812686106

Sheline, Y.I., Price, J.L., Yan, Z., Mintun, M.A., 2010. Resting-state functional MRI in depression unmasks increased connectivity between networks via the dorsal nexus. Proc. Natl. Acad. Sci. U. S. A. 107, 11020–11025. https://doi.org/10.1073/pnas.1000446107

Siddiqi, S.H., Trapp, N.T., Hacker, C.D., Laumann, T.O., Kandala, S., Hong, X., Trillo, L., Shahim, P., Leuthardt, E.C., Carter, A.R., Brody, D.L., 2019. Repetitive Transcranial Magnetic Stimulation with Resting-State Network Targeting for Treatment-Resistant Depression in Traumatic Brain Injury: A Randomized, Controlled, Double-Blinded Pilot Study. J. Neurotrauma 36, 1361–1374. https://doi.org/10.1089/neu.2018.5889

Siegle, G.J., Thompson, W.K., Collier, A., Berman, S.R., Feldmiller, J., Thase, M.E., Friedman, E.S., 2012. Toward Clinically Useful Neuroimaging in Depression Treatment: Prognostic Utility of Subgenual Cingulate Activity for Determining Depression Outcome in Cognitive Therapy Across Studies, Scanners, and Patient Characteristics. Arch. Gen. Psychiatry 69, 913. https://doi.org/10.1001/archgenpsychiatry.2012.65

Singh, A., Erwin-Grabner, T., Sutcliffe, G., Antal, A., Paulus, W., Goya-Maldonado, R., 2019. Personalized repetitive transcranial magnetic stimulation temporarily alters default mode network in healthy subjects. Sci. Rep. 9. https://doi.org/10.1038/s41598-019-42067-3

Speer, A.M., Kimbrell, T.A., Wassermann, E.M., D. Repella, J., Willis, M.W., Herscovitch, P., Post, R.M., 2000. Opposite effects of high and low frequency rTMS on regional brain activity in depressed patients. Biol. Psychiatry 48, 1133–1141. https://doi.org/10.1016/S0006-3223(00)01065-9

Stephanou, K., Davey, C.G., Kerestes, R., Whittle, S., Harrison, B.J., 2017. Hard to look on the bright side: neural correlates of impaired emotion regulation in depressed youth. Soc. Cogn. Affect. Neurosci. 12, 1138–1148. https://doi.org/10.1093/scan/nsx039

Stokes, M.G., Chambers, C.D., Gould, I.C., Henderson, T.R., Janko, N.E., Allen, N.B., Mattingley, J.B., 2005. Simple metric for scaling motor threshold based on scalp-cortex distance: application to studies using transcranial magnetic stimulation. J. Neurophysiol. 94, 4520–4527. https://doi.org/10.1152/jn.00067.2005

Strigo, I.A., Simmons, A.N., Matthews, S.C., Craig, A.D.B., Paulus, M.P., 2008. Association of major depressive disorder with altered functional brain response during anticipation and processing of heat pain. Arch. Gen. Psychiatry 65, 1275–1284. https://doi.org/10.1001/archpsyc.65.11.1275

Trivedi, M.H., Rush, A.J., Wisniewski, S.R., Nierenberg, A.A., Warden, D., Ritz, L., Norquist, G., Howland, R.H., Lebowitz, B., McGrath, P.J., Shores-Wilson, K., Biggs, M.M., Balasubramani, G.K., Fava, M., STAR*D Study Team, 2006. Evaluation of outcomes with citalopram for depression using measurement-based care in STAR*D: implications for clinical practice. Am. J. Psychiatry 163, 28–40. https://doi.org/10.1176/appi.ajp.163.1.28

Tustison, N.J., Avants, B.B., Cook, P.A., Yuanjie Zheng, Egan, A., Yushkevich, P.A., Gee, J.C., 2010. N4ITK: Improved N3 Bias Correction. IEEE Trans. Med. Imaging 29, 1310–1320. https://doi.org/10.1109/TMI.2010.2046908

Tziortzi, A.C., Haber, S.N., Searle, G.E., Tsoumpas, C., Long, C.J., Shotbolt, P., Douaud, G., Jbabdi, S., Behrens, T.E.J., Rabiner, E.A., Jenkinson, M., Gunn, R.N., 2014. Connectivity-Based Functional Analysis of Dopamine Release in the Striatum Using Diffusion-Weighted MRI and Positron Emission Tomography. Cereb. Cortex 24, 1165–1177. https://doi.org/10.1093/cercor/bhs397

Wang, L., An, J., Gao, H.-M., Zhang, P., Chen, C., Li, K., Mitchell, P.B., Si, T.-M., 2019. Duloxetine effects on striatal resting-state functional connectivity in patients with major depressive disorder. Hum. Brain Mapp. https://doi.org/10.1002/hbm.24601

Wang, Y., Yang, S., Sun, W., Shi, Y., Duan, H., 2016. Altered functional interaction hub between affective network and cognitive control network in patients with major depressive disorder. Behav. Brain Res. 298, 301–309. https://doi.org/10.1016/j.bbr.2015.10.040

Wang, Z., Wang, X., Liu, J., Chen, J., Liu, X., Nie, G., Jorgenson, K., Sohn, K.C., Huang, R., Liu, M., Liu, B., Kong, J., 2017. Acupuncture treatment modulates the corticostriatal reward circuitry in major depressive disorder. J. Psychiatr. Res. 84, 18–26. https://doi.org/10.1016/j.jpsychires.2016.09.014

Weigand, A., Horn, A., Caballero, R., Cooke, D., Stern, A.P., Taylor, S.F., Press, D., Pascual-Leone, A., Fox, M.D., 2018. Prospective Validation That Subgenual Connectivity Predicts Antidepressant Efficacy of Transcranial Magnetic Stimulation Sites. Biol. Psychiatry 84, 28–37. https://doi.org/10.1016/j.biopsych.2017.10.028

Williams, N.R., Sudheimer, K.D., Bentzley, B.S., Pannu, J., Stimpson, K.H., Duvio, D., Cherian, K., Hawkins, J., Scherrer, K.H., Vyssoki, B., DeSouza, D., Raj, K.S., Keller, J., Schatzberg, A.F., 2018. High-dose spaced theta-burst TMS as a rapid-acting antidepressant in highly refractory depression. Brain J. Neurol. https://doi.org/10.1093/brain/awx379

Wise, T., Marwood, L., Perkins, A.M., Herane-Vives, A., Joules, R., Lythgoe, D.J., Luh, W.-M., Williams, S.C.R., Young, A.H., Cleare, A.J., Arnone, D., 2017. Instability of default mode network connectivity in major depression: a two-sample confirmation study. Transl. Psychiatry 7, e1105.

Wolkenstein, L., Plewnia, C., 2013. Amelioration of cognitive control in depression by transcranial direct current stimulation. Biol. Psychiatry 73, 646–651. https://doi.org/10.1016/j.biopsych.2012.10.010

World Health Organization, 2017. Depression and Other Common Mental Disorders 1–24.

Yesavage, J.A., Fairchild, J.K., Mi, Z., Biswas, K., Davis-Karim, A., Phibbs, C.S., Forman, S.D., Thase, M., Williams, L.M., Etkin, A., O'Hara, R., Georgette, G., Beale, T., Huang, G.D., Noda, A., George, M.S., VA Cooperative Studies Program Study Team, 2018. Effect of Repetitive Transcranial Magnetic Stimulation on Treatment-Resistant Major Depression in US Veterans: A Randomized Clinical Trial. JAMA Psychiatry Chic. Ill. https://doi.org/10.1001/jamapsychiatry.2018.1483

Zaki, J., Davis, J.I., Ochsner, K.N., 2012. Overlapping activity in anterior insula during interoception and emotional experience. NeuroImage 62, 493–499. https://doi.org/10.1016/j.neuroimage.2012.05.012

Zhang, X., Huettel, S.A., Mullette-Gillman, O.A., Guo, H., Wang, L., 2019. Exploring common changes after acute mental stress and acute tryptophan depletion: Resting-state fMRI studies. J. Psychiatr. Res. 113, 172–180. https://doi.org/10.1016/j.jpsychires.2019.03.025

Zhang, Y., Brady, M., Smith, S., 2001. Segmentation of brain MR images through a hidden Markov random field model and the expectation-maximization algorithm. IEEE Trans. Med. Imaging 20, 45–57. https://doi.org/10.1109/42.906424

Zhu, X., Wang, X., Xiao, J., Liao, J., Zhong, M., Wang, W., Yao, S., 2012. Evidence of a dissociation pattern in resting-state default mode network connectivity in first-episode, treatment-naive major depression patients. Biol. Psychiatry 71, 611–617. https://doi.org/10.1016/j.biopsych.2011.10.035

Figures

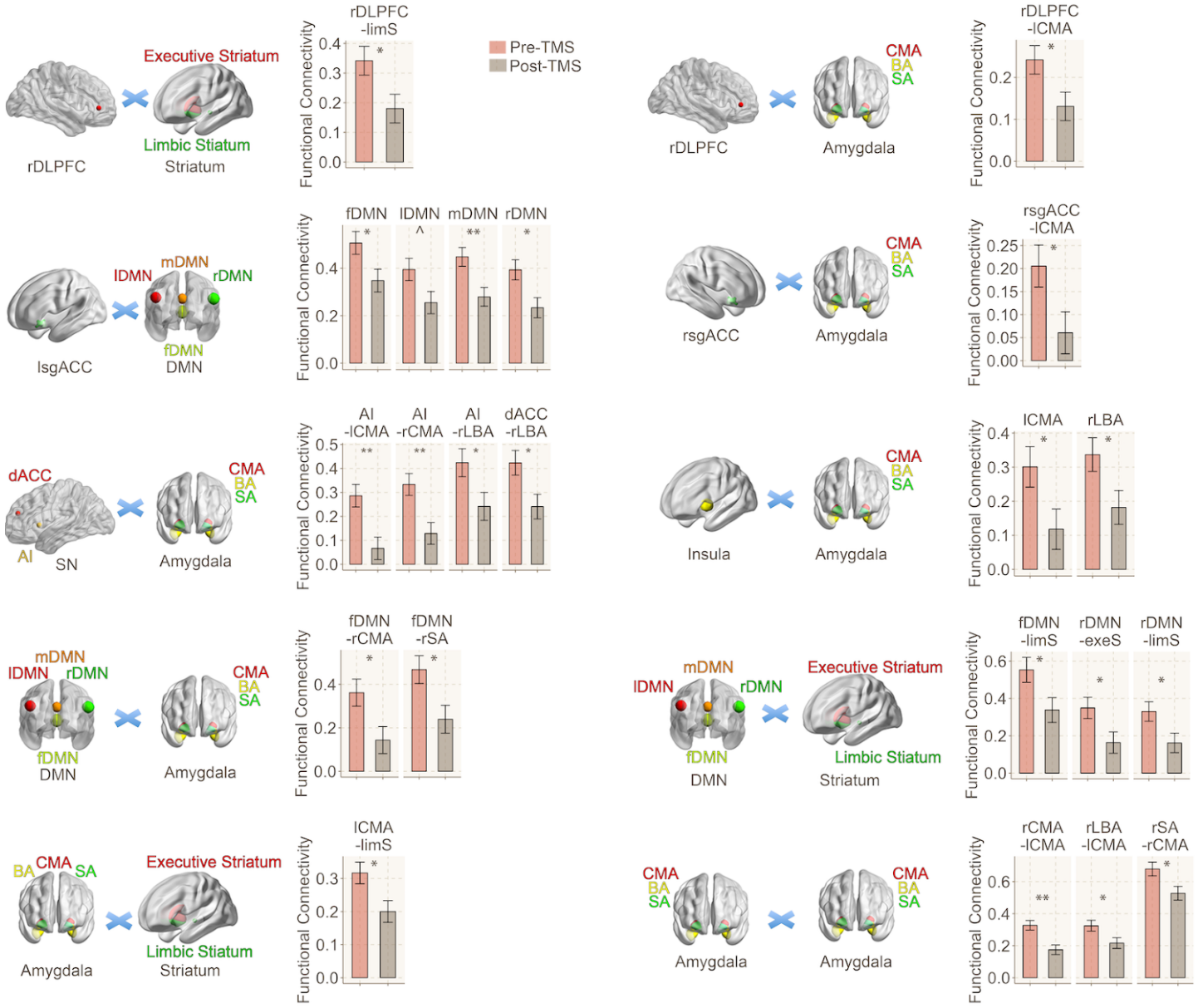

Figure 1. Statistically-significant changes in functional connectivity following SAINT in 18 participants with severe, treatment-resistant major depressive disorder. DLPFC: dorsolateral prefrontal cortex, sgACC: subgenual anterior cingulate cortex, DMN: default mode network, SN: salience network, dACC: dorsal anterior cingulate cortex, AI: anterior insula, CMA: centromedian amygdala, BA: basolateral amygdala, SA: superficial amygdala. Preceding r: right, preceding l: left. Paired t-tests were corrected for multiple comparisons using FDR ($q < .05$). Error bars indicate within-subject error. **q<.01, *q<.05, ^q=.06

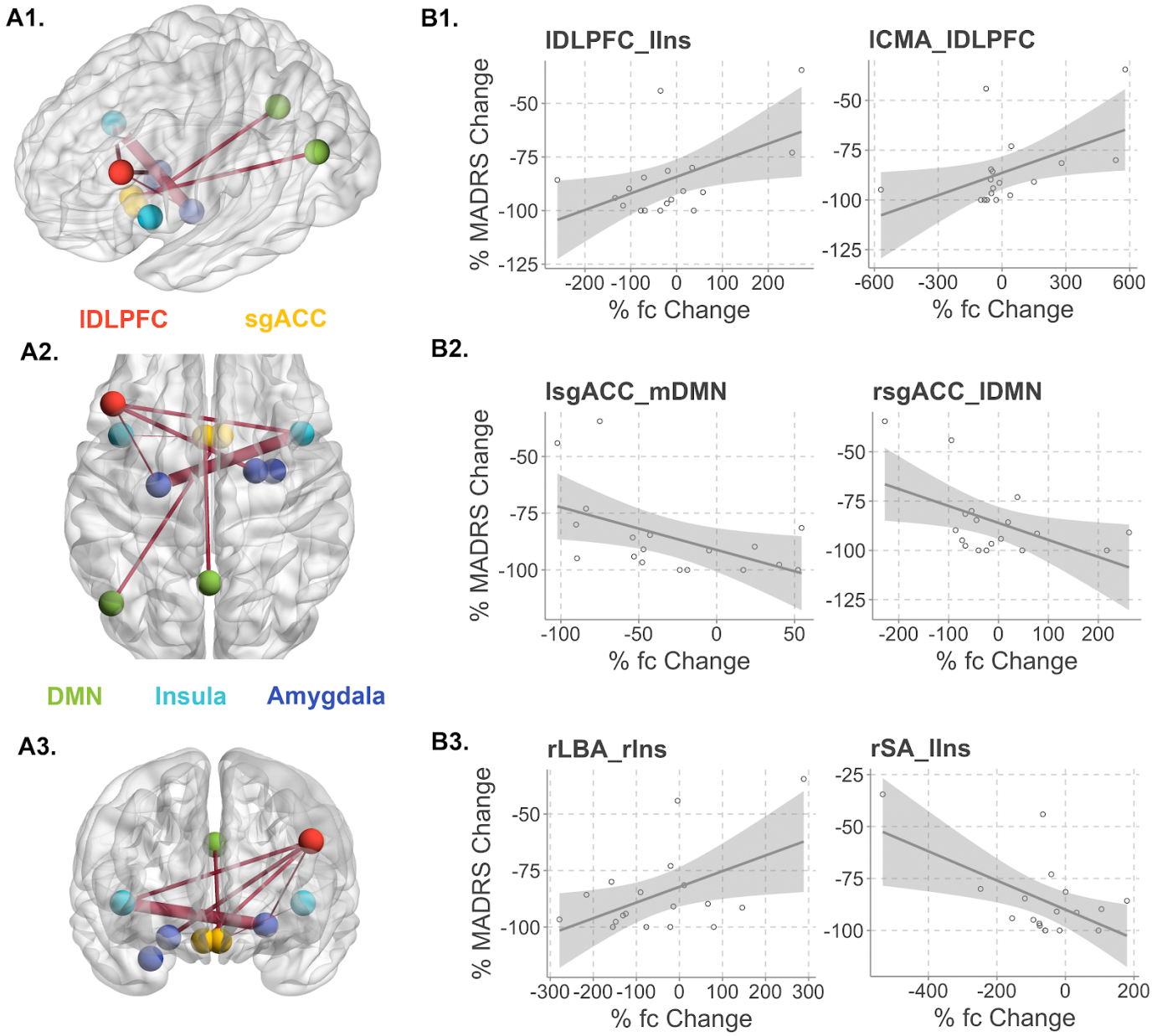

Figure 2. Statistically significant associations between changes in MADRS scores and fc changes following SAINT in 18 participants. **A**: Visualizations of the associations between changes in MADRS and changes in fc. The edges represent weighted R^2 values of the regression model - the greater the R^2, the thicker the edge. Nodes are coded by color with arbitrary size. **A1**: sagittal image, **A2:** axial image, **A3:** coronal image. **B:** Fc changes significantly associated with MADRS changes were observed between lDLPFC and insula, and amygdala subregions **(B1)**, between sgACC and DMN nodes **(B2)**, and between insula and amygdala subregions **(B3)**. Fc: functional connectivity, MADRS: Montgomery Asberg Depression Rating Scale, DLPFC: dorsolateral prefrontal cortex, sgACC: subgenual anterior cingulate cortex, DMN: default mode network, CMA: centromedian amygdala, BA: basolateral amygdala, SA: superficial amygdala. Preceding r: right, preceding l: left. The 95% confidence region is depicted by gray shading. All results were corrected for multiple comparisons using false discovery rate (q<.05). $\%\Delta = (postTreatment - baseline)/baseline * 100$

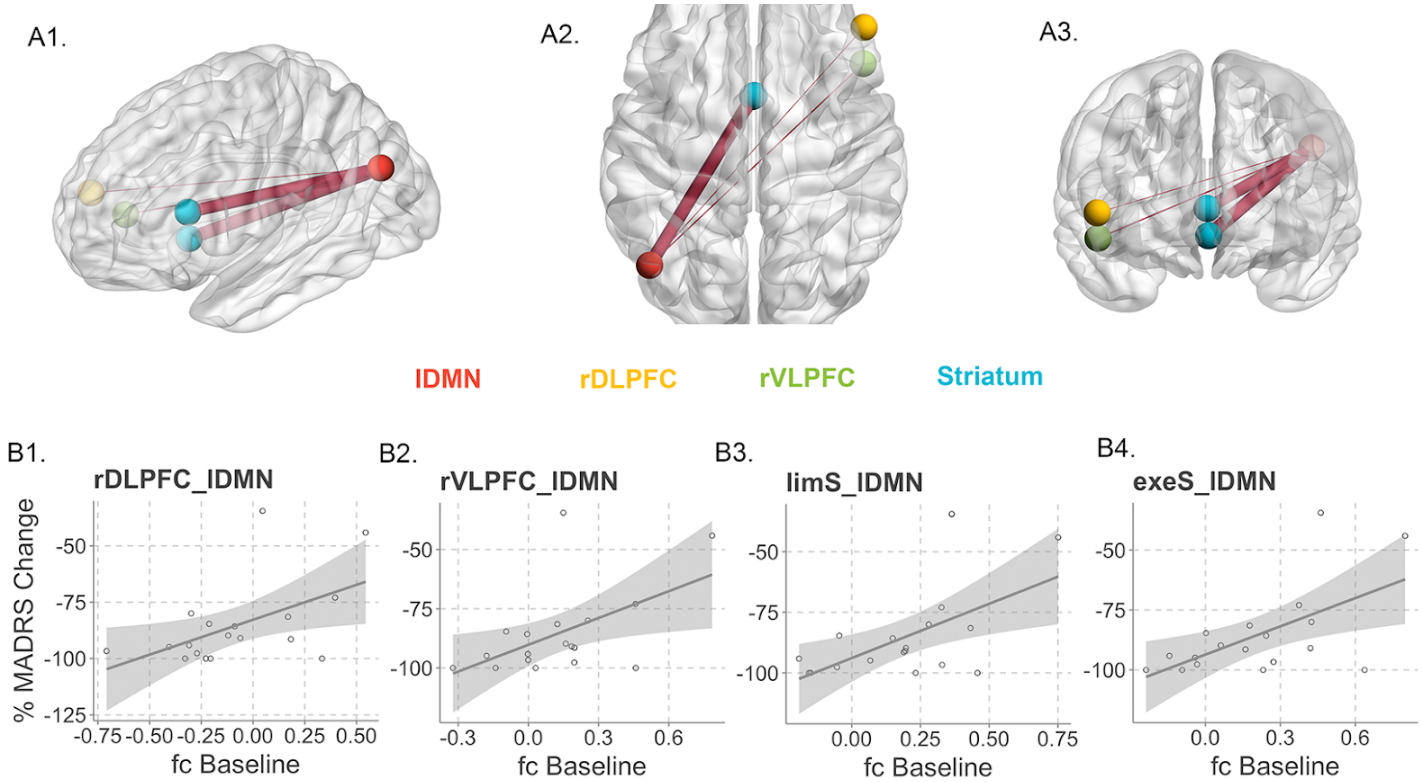

Figure 3. Baseline fc association with MADRS scores following SAINT. **A:** Visualizations of the associations between baseline fc and MADRS scores. The edges represents the weighted R^2 values of the regression model - the greater the R^2, the thicker the edge. Nodes are coded by color with arbitrary size. **A1:** sagittal image, **A2:** axial image, **A3:** coronal image. **B:** Baseline fc between lDMN and frontal cortex **(B1, B2)**, and between lDMN and striatum subregions **(B3, B4)** were significantly associated with MADRS changes. Fc: functional connectivity, MADRS: Montgomery Asberg Depression Rating Scale, DLPFC: dorsolateral prefrontal cortex, DMN: default mode network, VLPFC: ventrolateral prefrontal cortex, limS: limbic striatum, exeS: executive striatum. Preceding r: right, preceding l: left.The 95% confidence region is shaded gray. All results were corrected for multiple comparisons using false discovery rate (q<.05).

$$\%\Delta = (postTreatment - baseline)/baseline * 100$$

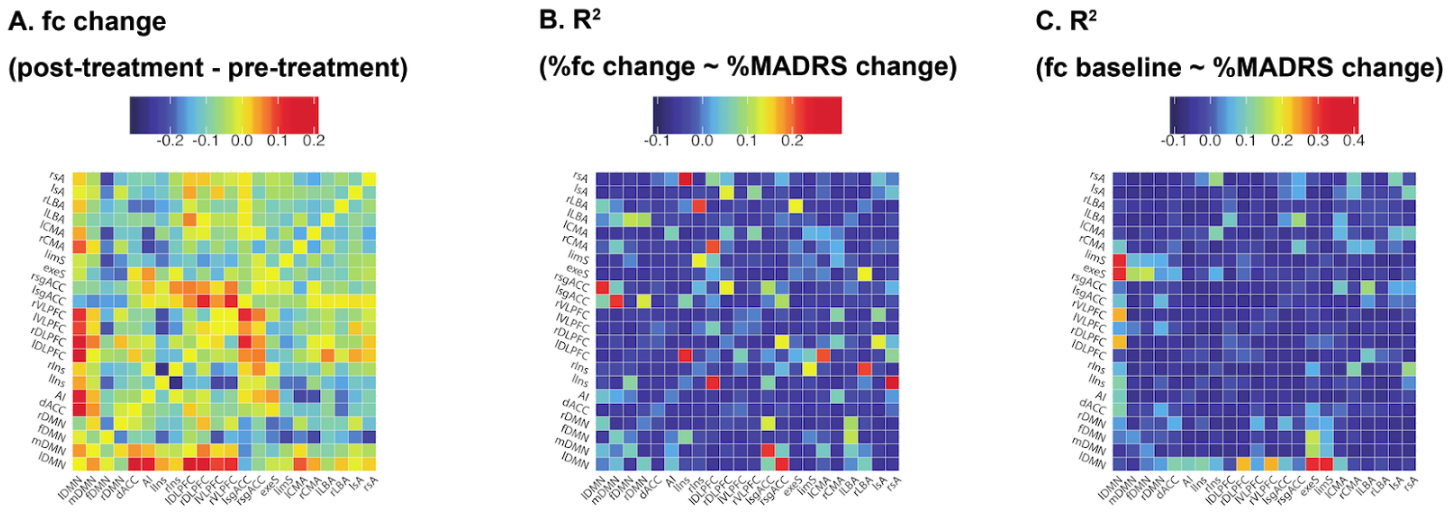

Figure S1. **A:** Functional connectivity changes ($\Delta = postTreatment - baseline$) between each pair of all 22 ROIs. **B**: Adjusted R^2 for the linear models relating functional connectivity changes to clinical score changes for each pair of all 22 ROIs. **C:** Adjusted R^2 for the linear models relating baseline functional connectivity to clinical score changes for each pair of all 22 ROIs.
$\%\Delta = (postTreatment - baseline)/baseline * 100$

Tables

Table S1. T-Test results for 16 responders (pre-treatment fc VS. post-treatment fc)

ROIs	t	ROIs	t	ROIs	t	ROIs	t	ROIs	t	ROIs	t	ROIs	t
lDMN_lDLPFC	***-2.187***	mDMN_rSA	0.567	rDMN_rCMA	1.74	AI_rCMA	***3.315***	rIns_rSA	1.583	lVLPFC_lLBA	0.483	exeS_rCMA	1.929
lDMN_lVLPFC	-2.052	fDMN_dACC	0.825	rDMN_rLBA	1.474	AI_rLBA	2.111	lDLPFC_lVLPFC	0.596	lVLPFC_lSA	-0.352	exeS_rLBA	1.904
lDMN_dACC	-1.982	mDMN_rCMA	1.094	rDMN_rsgACC	1.498	AI_rsgACC	-0.493	rIns_rCMA	***2.185***	lVLPFC_exeS	1.185	rsgACC_lSA	1.338
lDMN_rVLPFC	-1.691	fDMN_AI	1.47	rDMN_lSA	0.466	AI_lSA	2.01	lDLPFC_rVLPFC	0.091	lVLPFC_rSA	0.374	exeS_lSA	0.787
lDMN_lCMA	-1.607	fDMN_lVLPFC	1.355	dACC_lDLPFC	-0.443	lIns_lVLPFC	1.792	lDLPFC_lCMA	0.45	rVLPFC_lCMA	1.815	limS_rLBA	1.079
lDMN_rDLPFC	-1.51	fDMN_rDMN	1.187	rDMN_lLBA	1.669	AI_lLBA	1.585	lDLPFC_rDLPFC	0.05	lVLPFC_rLBA	1.151	exeS_lLBA	1.436
lDMN_AI	-1.186	mDMN_lLBA	1.029	rDMN_exeS	1.9	AI_exeS	-0.562	rIns_lLBA	0.569	lVLPFC_limS	1.176	rsgACC_rSA	0.861
lDMN_rCMA	-1.021	fDMN_rVLPFC	1.69	dACC_rDLPFC	0.123	lIns_rVLPFC	1.617	lDLPFC_rCMA	-0.07	rVLPFC_rCMA	1.064	limS_lSA	0.71
mDMN_rDLPFC	-0.939	rDMN_AI	0.667	dACC_rSA	1.125	rIns_rDLPFC	0.25	rDLPFC_rCMA	0.242	lsgACC_lSA	-0.624	lLBA_lSA	0.867
mDMN_dACC	-0.895	fDMN_lLBA	1.769	dACC_lCMA	1.49	lIns_lLBA	1.508	rDLPFC_lsgACC	-1.97	lsgACC_limS	0.623	rCMA_lLBA	1.326
mDMN_lVLPFC	-0.822	rDMN_lIns	0.829	AI_lIns	0.757	rIns_lVLPFC	1.612	rDLPFC_lLBA	-0.012	lsgACC_rSA	-0.385	lLBA_rSA	0.927
lDMN_lIns	-0.654	mDMN_rLBA	0.584	rDMN_limS	1.889	AI_limS	1.288	rIns_rLBA	1.799	lVLPFC_lCMA	0.615	exeS_limS	0.91
mDMN_rVLPFC	-0.642	rDMN_rIns	0.993	AI_rIns	-0.04	rIns_rVLPFC	1.252	rDLPFC_rLBA	0.787	rsgACC_exeS	0.506	rLBA_lSA	1.311
lDMN_mDMN	-0.557	mDMN_exeS	0.752	rDMN_lVLPFC	0.031	AI_lVLPFC	0.496	rIns_exeS	0.573	lVLPFC_rVLPFC	-0.659	rsgACC_rCMA	-0.105
mDMN_lDLPFC	-0.538	rDMN_dACC	-0.031	dACC_lSA	1.37	rIns_lDLPFC	1.124	rDLPFC_lCMA	1.986	lsgACC_rLBA	-0.236	lLBA_rLBA	1.419
lDMN_rLBA	-0.448	fDMN_rsgACC	1.459	dACC_rVLPFC	0.696	lIns_rsgACC	0.376	lDLPFC_rLBA	-0.029	rVLPFC_rLBA	1.334	lCMA_rCMA	***2.955***
lDMN_rIns	-0.373	mDMN_lSA	0.322	rDMN_lCMA	1.123	AI_lCMA	***3.102***	rIns_lSA	1.072	lVLPFC_rCMA	0.796	exeS_lCMA	0.702
lDMN_fDMN	-0.366	mDMN_limS	0.381	rDMN_rVLPFC	0.037	AI_rVLPFC	0.421	rIns_limS	1.631	lVLPFC_lsgACC	-0.817	rsgACC_lLBA	0.754
lDMN_rSA	-0.34	fDMN_limS	1.952	dACC_rsgACC	0.061	lIns_limS	1.983	lDLPFC_rSA	-0.718	rVLPFC_rSA	0.641	lCMA_rLBA	2.088
lDMN_exeS	-0.29	fDMN_lDLPFC	0.173	dACC_lIns	0.72	lIns_lDLPFC	1.356	lDLPFC_exeS	1.277	rVLPFC_exeS	0.602	limS_rCMA	0.255
mDMN_AI	-0.227	fDMN_rLBA	1.543	dACC_rCMA	1.416	lIns_rLBA	***2.24***	rDLPFC_rsgACC	-0.381	lsgACC_lCMA	0.733	rCMA_rLBA	1.564
lDMN_limS	-0.089	fDMN_rDLPFC	0.924	dACC_rIns	1.112	lIns_rDLPFC	2.006	lDLPFC_limS	1.217	rVLPFC_limS	1.606	limS_lLBA	1.287
lDMN_lSA	0.002	fDMN_exeS	1.332	dACC_lsgACC	0.199	lIns_exeS	0.59	lDLPFC_lSA	-0.726	rVLPFC_lSA	1.075	lCMA_lLBA	0.311
mDMN_rDMN	0.03	fDMN_rCMA	***2.16***	dACC_limS	0.657	lIns_rCMA	1.159	rDLPFC_rVLPFC	1.487	lsgACC_exeS	0.678	lCMA_rSA	1.366
mDMN_fDMN	0.152	fDMN_lCMA	1.821	dACC_exeS	-0.573	lIns_lCMA	1.84	rDLPFC_lVLPFC	-0.144	lsgACC_rsgACC	0.452	lCMA_lSA	0.609
mDMN_lIns	0.222	fDMN_lSA	2.156	dACC_lLBA	1.291	lIns_lSA	1.762	rDLPFC_exeS	1.111	lsgACC_rCMA	-0.317	rCMA_lSA	0.853
mDMN_rIns	0.271	fDMN_rSA	***2.463***	dACC_rLBA	2.103	lIns_rSA	2.132	rDLPFC_limS	***2.79***	lsgACC_lLBA	-0.39	rCMA_rSA	2.057
lDMN_lLBA	0.437	fDMN_lsgACC	2.036	dACC_lVLPFC	0.183	lIns_lsgACC	0.116	lDLPFC_lLBA	-1.566	rVLPFC_lLBA	0.81	limS_rSA	0.79
lDMN_rDMN	0.441	mDMN_lCMA	-0.126	rDMN_lsgACC	***2.577***	AI_lsgACC	-0.591	rIns_lCMA	1.055	lVLPFC_rsgACC	-0.186	rsgACC_rLBA	0.961
mDMN_rsgACC	0.967	rDMN_rDLPFC	-0.396	AI_rDLPFC	-0.283	rIns_rsgACC	-0.296	rDLPFC_rSA	-0.088	rsgACC_lCMA	***2.205***	lSA_rSA	0.611
lDMN_rsgACC	1.311	fDMN_rIns	1.51	dACC_AI	0.365	lIns_rIns	1.492	lDLPFC_rsgACC	-1.226	rVLPFC_rsgACC	-0.659	limS_lCMA	***2.306***
lDMN_lsgACC	2.043	fDMN_lIns	1.457	rDMN_rSA	2.143	AI_rSA	1.389	lDLPFC_lsgACC	-0.751	rVLPFC_lsgACC	-1.794	exeS_rSA	1.457
mDMN_lsgACC	***2.435***	rDMN_lDLPFC	0.271	AI_lDLPFC	-0.042	rIns_lsgACC	-0.18	rDLPFC_lSA	0.818	rsgACC_limS	0.219	rLBA_rSA	0.603

t values that are significant (q<.05) are in ***bold italics***.

Table S2. Linear regression results for 16 responders (%fc changes ~ %MADRS changes)

ROIs	Rsquare	ROIs	Rsquare	ROIs	Rsquare	ROIs	Rsquare	ROIs	Rsquare	ROIs	Rsquare	ROIs	Rsquare
mDMN_lDMN	0.122	lDLPFC_AI	-0.071	lsgACC_lDMN	0.109	exeS_lDLPFC	0.023	lCMA_lsgACC	-0.066	lLBA_lsgACC	-0.051	lSA_lDLPFC	-0.05
fDMN_lDMN	-0.071	lDLPFC_lIns	0.089	lsgACC_mDMN	0.086	exeS_rDLPFC	-0.018	lCMA_rsgACC	-0.019	lLBA_rsgACC	0.074	lSA_rDLPFC	-0.069
fDMN_mDMN	-0.038	lDLPFC_rIns	-0.069	lsgACC_fDMN	-0.065	exeS_lVLPFC	-0.022	lCMA_exeS	-0.053	lLBA_exeS	-0.019	lSA_lVLPFC	-0.052
rDMN_lDMN	0.072	rDLPFC_lDMN	-0.069	lsgACC_rDMN	-0.058	exeS_rVLPFC	-0.062	lCMA_limS	-0.064	lLBA_limS	0.039	lSA_rVLPFC	0.038
rDMN_mDMN	0.023	rDLPFC_mDMN	0.019	lsgACC_dACC	-0.066	exeS_lsgACC	-0.065	rCMA_lDMN	0.016	lLBA_lCMA	-0.053	lSA_lsgACC	-0.065
rDMN_fDMN	-0.071	rDLPFC_fDMN	-0.058	lsgACC_AI	0.012	exeS_rsgACC	-0.055	rCMA_mDMN	0.083	lLBA_rCMA	-0.071	lSA_rsgACC	-0.019
dACC_lDMN	-0.067	rDLPFC_rDMN	-0.04	lsgACC_lIns	0.007	limS_lDMN	-0.069	rCMA_fDMN	0.067	rLBA_lDMN	-0.049	lSA_exeS	0.076
dACC_mDMN	-0.054	rDLPFC_dACC	-0.03	lsgACC_rIns	-0.029	limS_mDMN	0.041	rCMA_rDMN	-0.019	rLBA_mDMN	-0.026	lSA_limS	-0.071
dACC_fDMN	-0.001	rDLPFC_AI	-0.062	lsgACC_lDLPFC	0.112	limS_fDMN	0.07	rCMA_dACC	-0.068	rLBA_fDMN	0.013	lSA_lCMA	0.03
dACC_rDMN	-0.01	rDLPFC_lIns	-0.07	lsgACC_rDLPFC	***0.231***	limS_rDMN	-0.071	rCMA_AI	-0.058	rLBA_rDMN	-0.002	lSA_rCMA	0.001
AI_lDMN	-0.035	rDLPFC_rIns	0.081	lsgACC_lVLPFC	-0.007	limS_dACC	-0.066	rCMA_lIns	-0.065	rLBA_dACC	-0.01	lSA_lLBA	-0.039
AI_mDMN	-0.051	rDLPFC_lDLPFC	-0.069	lsgACC_rVLPFC	-0.058	limS_AI	-0.066	rCMA_rIns	-0.058	rLBA_AI	-0.056	lSA_rLBA	-0.067
AI_fDMN	-0.062	lVLPFC_lDMN	0.069	rsgACC_lDMN	-0.049	limS_lIns	-0.025	rCMA_lDLPFC	-0.044	rLBA_lIns	-0.071	rSA_lDMN	-0.071
AI_rDMN	0.009	lVLPFC_mDMN	0.068	rsgACC_mDMN	-0.071	limS_rIns	0.034	rCMA_rDLPFC	-0.031	rLBA_rIns	-0.066	rSA_mDMN	-0.018
AI_dACC	-0.047	lVLPFC_fDMN	-0.053	rsgACC_fDMN	0.007	limS_lDLPFC	-0.043	rCMA_lVLPFC	-0.068	rLBA_lDLPFC	-0.071	rSA_fDMN	-0.071
lIns_lDMN	-0.04	lVLPFC_rDMN	-0.019	rsgACC_rDMN	-0.051	limS_rDLPFC	-0.068	rCMA_rVLPFC	0.069	rLBA_rDLPFC	0.114	rSA_rDMN	0.063
lIns_mDMN	-0.071	lVLPFC_dACC	0.005	rsgACC_dACC	-0.048	limS_lVLPFC	0.061	rCMA_lsgACC	-0.043	rLBA_lVLPFC	-0.071	rSA_dACC	-0.02
lIns_fDMN	-0.005	lVLPFC_AI	0.02	rsgACC_AI	0.05	limS_rVLPFC	-0.07	rCMA_rsgACC	0.041	rLBA_rVLPFC	-0.054	rSA_AI	-0.06
lIns_rDMN	-0.07	lVLPFC_lIns	0.003	rsgACC_lIns	0.042	limS_lsgACC	-0.022	rCMA_exeS	-0.027	rLBA_lsgACC	-0.025	rSA_lIns	-0.063
lIns_dACC	-0.031	lVLPFC_rIns	0.04	rsgACC_rIns	-0.071	limS_rsgACC	-0.055	rCMA_limS	***0.229***	rLBA_rsgACC	-0.068	rSA_rIns	0.048
lIns_AI	-0.07	lVLPFC_lDLPFC	-0.042	rsgACC_lDLPFC	0.05	limS_exeS	-0.054	rCMA_lCMA	-0.007	rLBA_exeS	0.193	rSA_lDLPFC	-0.071
rIns_lDMN	-0.009	lVLPFC_rDLPFC	0.027	rsgACC_rDLPFC	0.137	lCMA_lDMN	-0.066	lLBA_lDMN	-0.012	rLBA_limS	0.132	rSA_rDLPFC	-0.005
rIns_mDMN	-0.061	rVLPFC_lDMN	-0.05	rsgACC_lVLPFC	-0.069	lCMA_mDMN	-0.025	lLBA_mDMN	0	rLBA_lCMA	-0.032	rSA_lVLPFC	-0.032
rIns_fDMN	-0.036	rVLPFC_mDMN	-0.071	rsgACC_rVLPFC	0.026	lCMA_fDMN	-0.002	lLBA_fDMN	-0.064	rLBA_rCMA	-0.041	rSA_rVLPFC	-0.045
rIns_rDMN	-0.065	rVLPFC_fDMN	-0.043	rsgACC_lsgACC	0.168	lCMA_rDMN	-0.071	lLBA_rDMN	0.1	rLBA_lLBA	-0.054	rSA_lsgACC	-0.071
rIns_dACC	-0.071	rVLPFC_rDMN	-0.071	exeS_lDMN	-0.013	lCMA_dACC	-0.066	lLBA_dACC	0.085	lSA_lDMN	-0.055	rSA_rsgACC	0.094
rIns_AI	-0.046	rVLPFC_dACC	-0.061	exeS_mDMN	-0.069	lCMA_AI	-0.015	lLBA_AI	-0.043	lSA_mDMN	-0.057	rSA_exeS	0.09
rIns_lIns	-0.032	rVLPFC_AI	-0.07	exeS_fDMN	-0.002	lCMA_lIns	-0.062	lLBA_lIns	0.006	lSA_fDMN	-0.071	rSA_limS	0.031
lDLPFC_lDMN	-0.052	rVLPFC_lIns	-0.004	exeS_rDMN	-0.071	lCMA_rIns	0.017	lLBA_rIns	0.055	lSA_rDMN	0.04	rSA_lCMA	-0.046
lDLPFC_mDMN	-0.024	rVLPFC_rIns	-0.07	exeS_dACC	-0.07	lCMA_lDLPFC	0.185	lLBA_lDLPFC	0.059	lSA_dACC	-0.064	rSA_rCMA	-0.044
lDLPFC_fDMN	-0.071	rVLPFC_lDLPFC	0.119	exeS_AI	-0.069	lCMA_rDLPFC	0.053	lLBA_rDLPFC	0.127	lSA_AI	-0.064	rSA_lLBA	-0.071
lDLPFC_rDMN	-0.071	rVLPFC_rDLPFC	-0.066	exeS_lIns	0.022	lCMA_lVLPFC	-0.056	lLBA_lVLPFC	-0.017	lSA_lIns	0.036	rSA_rLBA	-0.012
lDLPFC_dACC	0.147	rVLPFC_lVLPFC	-0.014	exeS_rIns	-0.024	lCMA_rVLPFC	-0.06	lLBA_rVLPFC	-0.061	lSA_rIns	0.046	rSA_lSA	0.04

R^2 values that are significant (q<.05) are in ***bold italics***.

Table S3. Linear regression results for 16 responders (fc baseline ~ %MADRS changes)

ROIs	Rsquare	ROIs	Rsquare	ROIs	Rsquare	ROIs	Rsquare	ROIs	Rsquare	ROIs	Rsquare	ROIs	Rsquare
mDMN_lDMN	0.185	lDLPFC_AI	-0.069	lsgACC_lDMN	-0.069	exeS_lDLPFC	-0.047	lCMA_lsgACC	-0.065	lLBA_lsgACC	-0.049	lSA_lDLPFC	0.011
fDMN_lDMN	0.027	lDLPFC_lIns	0.064	lsgACC_mDMN	-0.063	exeS_rDLPFC	0.019	lCMA_rsgACC	0.029	lLBA_rsgACC	0.008	lSA_rDLPFC	-0.067
fDMN_mDMN	-0.068	lDLPFC_rIns	-0.041	lsgACC_fDMN	-0.04	exeS_lVLPFC	-0.071	lCMA_exeS	-0.071	lLBA_exeS	-0.04	lSA_lVLPFC	-0.048
rDMN_lDMN	***0.281***	rDLPFC_lDMN	0.119	lsgACC_rDMN	-0.042	exeS_rVLPFC	-0.01	lCMA_limS	0.002	lLBA_limS	-0.034	lSA_rVLPFC	-0.069
rDMN_mDMN	0.021	rDLPFC_mDMN	-0.063	lsgACC_dACC	-0.067	exeS_lsgACC	-0.071	rCMA_lDMN	-0.051	lLBA_lCMA	-0.025	lSA_lsgACC	-0.047
rDMN_fDMN	-0.07	rDLPFC_fDMN	-0.055	lsgACC_AI	0.022	exeS_rsgACC	-0.051	rCMA_mDMN	-0.071	lLBA_rCMA	-0.07	lSA_rsgACC	-0.017
dACC_lDMN	-0.025	rDLPFC_rDMN	-0.055	lsgACC_lIns	-0.067	limS_lDMN	0.079	rCMA_fDMN	-0.07	rLBA_lDMN	-0.058	lSA_exeS	0.044
dACC_mDMN	-0.045	rDLPFC_dACC	-0.011	lsgACC_rIns	-0.028	limS_mDMN	-0.064	rCMA_rDMN	-0.066	rLBA_mDMN	-0.066	lSA_limS	0.073
dACC_fDMN	-0.047	rDLPFC_AI	0.002	lsgACC_lDLPFC	0.026	limS_fDMN	-0.049	rCMA_dACC	-0.034	rLBA_fDMN	0.043	lSA_lCMA	0.03
dACC_rDMN	-0.067	rDLPFC_lIns	0.031	lsgACC_rDLPFC	-0.054	limS_rDMN	-0.071	rCMA_AI	0.011	rLBA_rDMN	-0.061	lSA_rCMA	-0.034
AI_lDMN	-0.006	rDLPFC_rIns	0.019	lsgACC_lVLPFC	-0.068	limS_dACC	-0.071	rCMA_lIns	0.053	rLBA_dACC	-0.05	lSA_lLBA	-0.061
AI_mDMN	-0.07	rDLPFC_lDLPFC	-0.057	lsgACC_rVLPFC	-0.068	limS_AI	-0.048	rCMA_rIns	-0.004	rLBA_AI	0.056	lSA_rLBA	-0.06
AI_fDMN	-0.045	lVLPFC_lDMN	-0.07	rsgACC_lDMN	-0.063	limS_lIns	-0.024	rCMA_lDLPFC	-0.019	rLBA_lIns	-0.044	rSA_lDMN	0.024
AI_rDMN	-0.071	lVLPFC_mDMN	-0.069	rsgACC_mDMN	0.028	limS_rIns	-0.071	rCMA_rDLPFC	-0.017	rLBA_rIns	-0.006	rSA_mDMN	-0.071
AI_dACC	-0.01	lVLPFC_fDMN	-0.062	rsgACC_fDMN	-0.056	limS_lDLPFC	0.032	rCMA_lVLPFC	-0.05	rLBA_lDLPFC	0.125	rSA_fDMN	-0.031
lIns_lDMN	-0.031	lVLPFC_rDMN	-0.024	rsgACC_rDMN	0.006	limS_rDLPFC	0.052	rCMA_rVLPFC	-0.026	rLBA_rDLPFC	0.069	rSA_rDMN	-0.071
lIns_mDMN	-0.051	lVLPFC_dACC	-0.064	rsgACC_dACC	-0.008	limS_lVLPFC	-0.063	rCMA_lsgACC	-0.059	rLBA_lVLPFC	-0.008	rSA_dACC	0.023
lIns_fDMN	-0.013	lVLPFC_AI	-0.067	rsgACC_AI	0.081	limS_rVLPFC	-0.061	rCMA_rsgACC	-0.067	rLBA_rVLPFC	-0.027	rSA_AI	0.098
lIns_rDMN	-0.053	lVLPFC_lIns	-0.019	rsgACC_lIns	-0.062	limS_lsgACC	0.075	rCMA_exeS	-0.071	rLBA_lsgACC	-0.032	rSA_lIns	0.125
lIns_dACC	-0.056	lVLPFC_rIns	-0.022	rsgACC_rIns	-0.042	limS_rsgACC	0.026	rCMA_limS	-0.057	rLBA_rsgACC	0.046	rSA_rIns	0.098
lIns_AI	-0.071	lVLPFC_lDLPFC	-0.056	rsgACC_lDLPFC	0.068	limS_exeS	-0.063	rCMA_lCMA	-0.044	rLBA_exeS	0.15	rSA_lDLPFC	***0.228***
rIns_lDMN	-0.055	lVLPFC_rDLPFC	-0.07	rsgACC_rDLPFC	-0.071	lCMA_lDMN	-0.035	lLBA_lDMN	0.011	rLBA_limS	0.118	rSA_rDLPFC	0.033
rIns_mDMN	-0.011	rVLPFC_lDMN	0.117	rsgACC_lVLPFC	-0.071	lCMA_mDMN	-0.023	lLBA_mDMN	-0.063	rLBA_lCMA	-0.04	rSA_lVLPFC	0.071
rIns_fDMN	-0.013	rVLPFC_mDMN	-0.051	rsgACC_rVLPFC	-0.071	lCMA_fDMN	-0.02	lLBA_fDMN	-0.027	rLBA_rCMA	-0.065	rSA_rVLPFC	0.002
rIns_rDMN	-0.002	rVLPFC_fDMN	-0.057	rsgACC_lsgACC	-0.069	lCMA_rDMN	-0.065	lLBA_rDMN	-0.062	rLBA_lLBA	-0.061	rSA_lsgACC	-0.043
rIns_dACC	-0.071	rVLPFC_rDMN	-0.032	exeS_lDMN	0.038	lCMA_dACC	-0.013	lLBA_dACC	-0.07	lSA_lDMN	-0.065	rSA_rsgACC	0.114
rIns_AI	-0.071	rVLPFC_dACC	-0.028	exeS_mDMN	-0.057	lCMA_AI	0.044	lLBA_AI	-0.048	lSA_mDMN	-0.053	rSA_exeS	***0.21***
rIns_lIns	-0.025	rVLPFC_AI	0.002	exeS_fDMN	-0.071	lCMA_lIns	-0.03	lLBA_lIns	-0.07	lSA_fDMN	-0.041	rSA_limS	0.095
lDLPFC_lDMN	-0.057	rVLPFC_lIns	0.066	exeS_rDMN	-0.064	lCMA_rIns	0.025	lLBA_rIns	-0.047	lSA_rDMN	-0.069	rSA_lCMA	-0.051
lDLPFC_mDMN	-0.065	rVLPFC_rIns	0.071	exeS_dACC	-0.071	lCMA_lDLPFC	0.13	lLBA_lDLPFC	-0.041	lSA_dACC	-0.032	rSA_rCMA	-0.026
lDLPFC_fDMN	-0.019	rVLPFC_lDLPFC	-0.053	exeS_AI	-0.071	lCMA_rDLPFC	0.066	lLBA_rDLPFC	-0.058	lSA_AI	-0.019	rSA_lLBA	-0.071
lDLPFC_rDMN	0.005	rVLPFC_rDLPFC	-0.065	exeS_lIns	0.012	lCMA_lVLPFC	-0.021	lLBA_lVLPFC	-0.058	lSA_lIns	-0.036	rSA_rLBA	-0.058
lDLPFC_dACC	-0.071	rVLPFC_lVLPFC	-0.065	exeS_rIns	-0.019	lCMA_rVLPFC	0.033	lLBA_rVLPFC	-0.071	lSA_rIns	-0.045	rSA_lSA	-0.005

R^2 values that are significant (q<.05) are in ***bold italics***.